DYNAMICS IN CONCENTRATED COLLOIDAL SUSPENSIONS

Nikoleta Borissova Simeonova

Universiteit Utrecht

This work is part of the research program of the Council for Chemical Science (CW)

On the cover: Bond of Union by M.C. Escher, 1956

ISBN: 97-890-393-49-663
Printed by : Drukkerij Houx Digiprint, Maastricht, October 2008

DYNAMICS IN CONCENTRATED COLLOIDAL SUSPENSIONS

Dynamica in geconcentreerde colloïdale suspensies

(met een samenvatting in het Nederlands)

Динамика в концентрирани колоидни суспензии

(с кратко резюме на Български)

Proefschrift

ter verkrijging van de graad van doctor aan de Universiteit Utrecht op gezag van de rector magnificus, prof.dr. J.C. Stoof, ingevolge het besluit van het college voor promoties in het openbaar te verdedigen op woensdag 26 november 2008 des ochtends te 10.30 uur

door

Nikoleta Borissova Simeonova
geboren op 2 april 1976, te Sofia, Bulgarije

Promotor: Prof.dr. W.K.Kegel

This thesis was accomplished with the financial support of the Netherlands Organization for Scientific Research (NWO)

На моето семейство

Content

"True wisdom comes to each of us when we realize how little we understand about life, ourselves, and the world around us."
Socrates

1

General Introduction

1.1 Colloids as model system

The origin of colloid science can be dated back to 1845, when the Italian chemist and toxicologist Francesco Selmi described the first examples of colloidal particles. He defined the common properties of solutions such as silver chloride, sulfur and Prussian blue in water, and named them "pseudo solutions" [1] (for the original papers see [2,3,4,5,6]). In 1861 Thomas Graham introduced the term "colloid" [7] (from the Greek "kolla", which means "glue") to describe Selmi's "pseudo solutions". This term emphasizes their low rate of diffusion – a few orders of magnitude smaller, compared to the one of molecularly soluble substances. Based on this small diffusion rate, Graham concluded a lack of spontaneous crystallization in colloidal solutions. Further research, however, showed that such connection does not exist and probably, the low diffusion rates of colloids are caused by their relatively large size - at least 1 nm in diameter.

In 1827 English botanist Robert Brown observed under a microscope a suspension of pollen grains in water and noticed that they experience a permanent motion [8, 9].This phenomenon was later called after him - Brownian motion and was defined as a property of a particle to move equally likely in any direction in space as any further motion is unrelated to the previous one.

In 1905-1906 Einstein and Smoluchowski, independently, gave the first quantitative theory of the Brownian motion [10], which later was confirmed by Perrin [11] and Svedberg.

Trajectories of particles with diameter of half a micron, subject to Brownian motion, are illustrated in Figure 1-1 [11].

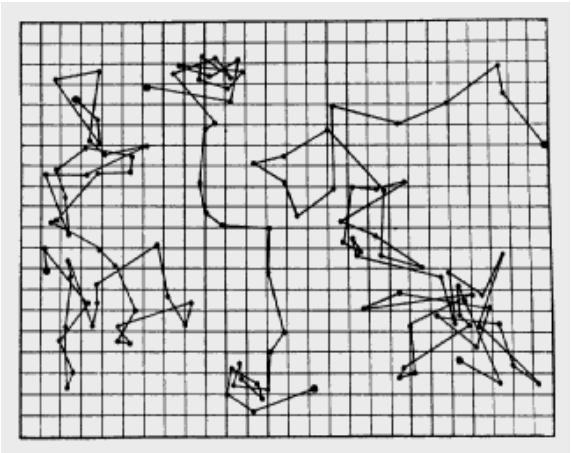

Figure1-1 Reproduced from the book of Perrin [11], three tracings of the motion of colloidal particles of radius 0.53μm, as seen under the microscope. Successive positions every 30 seconds are joined by straight line (the mesh size is 3.2μm).

Nowadays it is known that Brownian motion can be observed in colloidal systems with sizes up to several microns [12].

Brownian motion gives rise to 'diffusion' as described by eq. (1.1), i.e., mean-square displacement of particles that is proportional to time with proportionality constant the diffusion coefficient. The equation that gives the relation between the diffusion coefficient D and particle size or viscosity of the media is Einstein equation and has the form:

$$D = \frac{kT}{B}, \tag{1.1}$$

were k is Boltzmann`s constant $k=1.38*10^{-23}\ JK^{-1}$, T- absolute temperature and B is a friction coefficient for the colloid particle in the medium. For spherical particles with radius r and viscosity of the medium η, $B=6\pi\eta r$ (Stokes relation). Measuring the diffusion rates and calculating the diffusion coefficients of colloidal systems became one of the main methods for determination of particle size.

The fundamental time scale used in colloidal science is the Brownian time, τ_B, defined as the time it takes for an infinitely diluted particle to diffuse over its own radius, i.e.,

$$\tau_{\mathrm{B}} = \frac{r^2}{6D_0}, \tag{1.2}$$

where D_0 is the diffusion coefficient at infinite dilution being on the order of 10^{-13} – 10^{-12} m^2/s, depending on the solvent viscosity. All the experimental times in this thesis are converted in to Brownian time units in order to compare data obtained for systems with different particle sizes and solvent viscosity.

In the second half of last century it was found that the behavior of colloids in a solvent is thermodynamically equivalent to the one of atoms and molecules [13]. This property allows using colloids as a model experimental system for experiments on macro scale, which can confirm or reject theories with respect to micro world. An experimental advantage of colloids is their relatively big size (in comparison to the atoms and molecules) and, as a consequence from that, a typical time-scale on which colloidal processes take place. For example, the time-scale on which a particle with radius 500 nm in a dilute suspension diffuses a distance equal to its own radius, is 0.5 s. Such time scale allows a real time analysis to be performed, using well known and accessible experimental techniques such as optical microscopy and light scattering.

At present times colloidal systems find also very broad application in industry as a basic material for many products. Colloids are widely used in our daily life. In food industry they are present in products such as milk, cheese and mayonnaise; colloids are used in home and body care industry - for all types of detergents and beauty products; coatings and paints. In oil industry, colloidal particles are used in drilling processes. About 25 years ago first steps in a new field of application of colloids were made – colloids in medicine. In modern medical research, colloidal particles are widely used for cell- and DNA-separation, in in-vitro diagnostics, proteomics and as drug carriers [14, 15, 16, 17]. This wide application range determines the high demand for better understanding of colloidal behavior.

1.2 Scope of this thesis

An interesting property of colloids is that in suspension they show transitions between fluid-, solid-, and glass- like phases [18], similar to atoms and molecules. As there are no energetic contributions to the free-energy of a hard-sphere system, the occurrence of a phase transition in this system would be driven by entropy [19]. The first results that described a freezing transition in a hard-sphere system were obtained by computer simulations by Wood and

Jacobson and Alder and Wainwright [20, 21]. The first experimental results indicating the existence of a phase transition driven by entropy were presented by Hachisu, Kobayashi and Kose [22, 23].The phase behavior of colloids that interact as hard-spheres was later confirmed by Pusey and van Megen [24], who also described a so called “glass transition”. This transition can occur when a colloidal system is quenched (for example by centrifugation) to high-volume fractions of particles [25, 26]. In quenched colloidal system particles are trapped in a disordered state and the system is referred to as “colloidal glass”. Such a system is characterized by lack of long range order of the particles and caging of a single particle by its neighbors. Glass transition occurs at volume fractions of particles above 0.58. However, recent computer simulations [27] and experiments [28] show that monodisperse [27] but also 5% polydisperse [29] hard spheres crystallize in the absence of gravity up to volume fractions close to 0.64. In the last study, a system that is a glass on earth rapidly crystallizes in space (in absence of gravity) after homogenization by mixing. These observations question the very existence of a glass transition at volume fractions of particles below 0.64 in the absence of a gravity field. However, no quantitative studies of the influence of gravity on dynamics in concentrated colloidal suspensions have been reported. In Chapters 4 and 6 of this thesis, the question as to what the influence of gravity is on particle mobility (quantified by the mean squared displacement) in glassy systems is addressed.

Another topic included in this thesis is the “devitrification” of colloidal glasses, discussed in Chapter 5.

The presence of non adsorbing polymer in a colloidal system induces a short - range attraction, called depletion interaction [29]. The mass centers of polymer coils of radius of gyration r_g is expelled from a zone of width r_g from the surface of each colloid, so called depletion zone. When two colloids approach each other so that their depletion zones overlap, the polymers in the system are excluded from overlap volume and this result in an imbalance in polymer osmotic pressure, which pushes particles together. The model system is presented in Figure 1-2. This depletion interaction is well described by Asakura-Oosawa [29] and A.Vrij [27]. Its dimensionless range can be estimated by the size ratio $q= r_g/r$, where r_g is the radius of gyration of the polymer and r is the radius of the particle and its strength is proportional to the concentration of polymer coils in the free volume available to them. The effective interaction potential, U, is given by

$$U = \begin{cases} \infty & R < \sigma_c \\ -\Pi V_{overlap} & \sigma_c < R < \sigma_c + \sigma_p \\ 0 & r > \sigma_c + \sigma_p \end{cases}$$

where Π is the osmotic pressure due to the polymer presence, $V_{overlap}$ the overlap volume of the depletion zones, R the distance between the particles centers, $\sigma_c=2r$ the diameter of the particle and $\sigma_p=2r_g$ the diameter of the polymer coil [30]. At low polymer concentration, the thickness of the depletion zone can be considered as equal to the radius of gyration, r_g, of polymer coil.

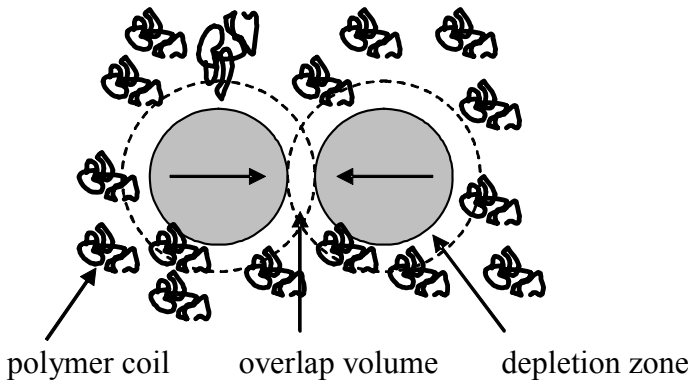

Figure 1-2 Mechanism of the depletion interaction

The concentration (volume fraction) of polymer in the system can be used as a variable to describe the colloid-polymer mixture systems. Adding a non adsorbing polymer to colloidal glasses can promote so called “devitrification” [31, 32, 33]. ’Devitrification’ is when structurally disordered systems that do not reach long-time self diffusion within the experimental time scales do so after introducing attraction. Interestingly, the system again forms a glass state and the process is called reentrant glass transition. If even more polymer is added so called attractive glass is formed. In Chapter 5 is shown that the process is accompanied by significant changes in the displacement distribution and its moments. However, no significant variations have been detected in the shapes of the displacement distributions. Moreover, it is shown, that structural correlation functions and the magnitude

of local density fluctuations do not vary significantly between the glass states and the fluid state.

This thesis ends with a short summary translated in Dutch and Bulgarian languages.

References

[1]. A. Sheludko, КолоиднаХимия, Наука и изкуство, Sofia 1957
[2]. F. Selmi, Intorno all'azione dell'iodio sopra il clorido di mercurio : memoria prima di Francesco Selmi, Milano: V. Guglielmini, (1845)
[3]. F. Selmi, Azione del latte sulle materie metalliche e reazioni di queste su quello: discorso letto da Francesco Selmi nell'adunanza pubblica del 21 maggio 1847 della Societa d'agricoltura di Reggio, Modena: Antonio ed Angelo Cappelli, (1847)
[4]. F. Selmi, Intorno ai vocaboli precipitazione e coagulazione adoprati indistintamente a significare il deporsi dell'albumina da un menstruo allo stato insolubile: considerazioni presentate alla R. Accademia di Scienze, Lettere ed Arti di Modena nell'adunanza del 30 marzo 1842, e lette nel congresso scientifico italiano riunitosi in Padova nel settembre dello stesso anno da Francesco Selmi, Modena: Pei Tipi della R.D. Camera, (1843)
[5]. F. Selmi, Studj sulla dimulsione di cloruro d'argento, Nuovi Annali delle Scienze Naturali di Bologna, fasc. di agosto (1845)
[6]. F. Selmi, Studio intorno alle pseudo-soluzioni degli azzurri di Prussia ed alla influenza dei sali nel guastarle, Bologna: Tipi Sassi, (1847)
[7].T.Graham, Liquid Diffusion Applied to Analysis Philosophical Transactions of the Royal Society of London, 151, 183-224, (1861)
[8]. R. Brown, A brief Account of Microscopical Observations made in the Months of June, July, and August, 1827, on the Particles contained in the Pollen of Plants; and on the general Existence of active Molecules in Organic and Inorganic Bodies, Philos. Mag. N. S. 4 161-173, (1828)
[9]. R.Brown, Additional Remarks on Active Molecules, Philos. Mag. N. S. 6, 161-166,(1829)
[10].A. Einstein, Über die von der molekularkinetischen Theorie der Wärme geforderte Bewegung von in ruhenden Flüssigkeiten suspendierten Teilchen, Ann. Phys., 17, 549, (1905)
[11]. J. Perrin, Ann. Chem. Phys, 18, 1, (1909)
[12]. G. Bosma, et al, J. Colloid Interface Sci., 245, 292-300, (2002)
[13]. A. Vrij, E. A. Nieuwenhuis, et all, Faraday Discuss., 65, 101-113, (1978)
[14]. A.K.Gupta, M.Gupta, Biomaterials, 26, 3995–4021, (2005)
[15]. M.Fuentes, et al, Biosensors and Bioelectronics, 20, 1380–1387, (2005)
[16]. D.Muller-Schulte, M.Hodenius, Radiation Phys. Chem., 63, 513–516, (2002)
[17]. C.Barbe, et al, Adv.Mater.,16, 1959-1966, (2004)
[18]. P. N. Pusey, Liquids, freezing, and the glass transition, Elsevier, Amsterdam, (1990).
[19]. L.Onsager, Phys.Rev ,65, 117, (1944)
[20]. W. W. Wood and J. D. Jacobson, J. Chem. Phys., 27, 1207-1208, (1957)
[21]. B. J. Alder and T. E. Wainwright, J.Chem. Phys., 27, 1208-1209, (1957)
[22]. S. Hachisu, Y. Kobayashi, and A. Kose, J. Colloid Interface Sci., 42, 342-348, (1973)
[23]. S. Hachisu and Y. Kobayashi, Kirkwood-Alder, J. Colloid Interface Sci., 46, 470-476, (1974)
[24]. P. N. Pusey and W. van Megen, Nature, 320, 340, (1986)

[25]. P.G.Debenedetti,Metastable liquids,Princeton Univ.press,Princeton, NJ, (1996)
[26]. P. N. Pusey and W. Van Megen, Phys. Rev. Lett., 59, 2083-2086, (1987)
[27]. M.D. Rintoul and S. Torquato, Phys. Rev. Lett., 77, 4198, (1996)
[28]. J. Zhu, M. Li, R. Rogers, W. Meyer, R.H. Ottewill, Crew-Shuttle Columbia, W.B. Russel, and P.M. Chaikin, Nature., 387, 883, (1997)
[29]. S. Asakura and F. Oosawa, J. Chem. Phys., 22, 1255-1256, (1954)
[30]. A. Vrij, Pure Appl. Chem., 48, 471, (1976)
[31]. K. Dawson, G. Foffi, M. Fuchs, W. Gotze, F. Sciortino, M. Sperl, P. Tartaglia, T. Voigtmann, and E. Zaccarelli, Phys. Rev. E, 63, 011401, (2000)
[32]. K. N. Pham, A. M. Puertas, J. Bergenholtz, S. U. Egelhaaf,A. Moussad, P. N. Pusey, A. B. Schofield, M. E.Cates, M. Fuchs, and W. C. K. Poon, Science, 296, 104,(2002)
[33]. T. Eckert and E. Bartsch, Phys. Rev. Lett., 89, 125701,(2002)

2

Experimental technique

2.1 Confocal Scanning Laser Microscopy

The main advantage of colloids as model experimental system is their relatively large size and long time-scale for diffusion. With respect to that, optical analytical methods are widely employed for studying colloidal systems. One of the most used techniques is light microscopy as it allows obtaining images on which real space analysis can be performed.

In a conventional light microscope, the entire sample is illuminated via transmitted white light. The resulting image suffers of low contrast and low resolution (the ability to distinguish two objects) due to the blur of out of focus objects. Because of this, the conventional light microscopy is not applicable for studying systems with high colloidal concentrations such as glasses or colloidal crystals where the distances between particles are comparable to the microscope resolution distance. In these cases a sequential imaging of single focal points in one plain is required in order to filter out of focus light. In this aspect, Confocal Scanning Laser Microscopy (CSLM) is one of the methods that offer several advantages over conventional optical microscopy, including controllable depth of field, the elimination of image degrading out of focus light, and the ability to collect serial optical sections from thick specimens.

Confocal imaging was invented by Marvin Minsky, patented in 1957 [1] and is employed in all modern confocal microscopes. The method of image formation in a confocal microscope is fundamentally different from the one of usual light microscope. Illumination is achieved by scanning one or more focused beams of light, usually from a laser, across the sample. This point of illumination is brought to focus in the sample by the objective lens, and laterally scanned using scanning device. The sequences of points of light from the sample are detected by a photomultiplier tube through a pinhole, and the output from the photomultiplier is built into an image and displayed.

Originally confocal microscopy was mainly applied as analytical method in biology for studying cell cultures [2, 3, 4, 5]. In colloidal science confocal microscopy was introduced as advanced method for 3D analysis. One of the first studied objects were colloidal crystals [6].

Although samples of colloids can be viewed using light reflected back from the sample, colloidal particles are usually labeled with fluorescent die in order to achieve high resolution. Some colloidal particles can be composed of fluorescent core and nonfluorescent shell. Such particles, dispersed in refractive index matched solvent allow a 3D analysis to be performed on single particle level [7, 8], since in this case particles fluorescent cores are separated by a distance which is at least on the order of the optical resolution. Recent quantitative analyses were done in terms of static and dynamic correlation functions [9, 10, 11]. An example image of fluorescently labeled particles in fluid and crystal phase is shown in Figure 2-1.

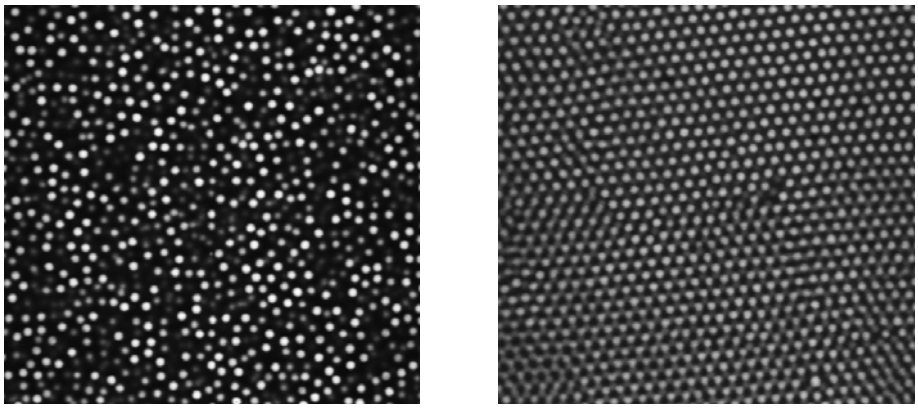

Figure 2-1 Example of CSLM image of samples of fluorescently labeled colloidal particles. Left - fluid phase, right– crystal phase

Technically, confocal microscope differs from the regular bright field light microscope by the presence of two pinholes. One of these pinholes is placed in the back focal plane of the objective in front of the light source – source pinhole. The other pinhole is placed in the focal plane in front of the detector – detector pinhole. A sketch of confocal scanning laser microscope (CSLM) optical pathway is shown in Figure 2-2. The detector can be a point detector, usually a photo multiplier tube. Light excited in the sample in the focal point of the objective is imaged in the opening of the detector pinhole and light that is excited from points in the sample outside a small region around the focal point is blocked by the detector pinhole. This is how a single point anywhere in a 3D sample can be accurately imaged. By scanning this point laterally through the focal plane, a 2D image of a slice through the sample can be made. For a fluorescently labeled sample with the refractive index of the particles matched with respect to the solvent refractive index, the depth of imaging is only limited by the working distance of the objective.

With the use of a high numerical aperture lens this distance is a few hundred micrometers. The source pinhole, placed in front of the light source, is to create a point source. This point source is focused to a diffraction-limited spot in the sample.

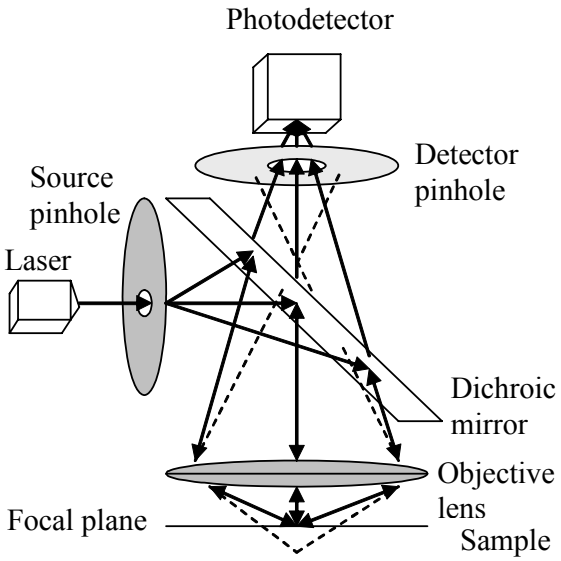

Figure 2-2 Schematic image of the operating principle of a confocal microscope. The straight lines indicate the path followed by excitation and detected emission light (assuming fluorescence microscopy). The dashed lines indicate the beam path of light generated by an out of focus source, which is effectively rejected by the pinhole aperture of the point-detector.

Regardless of the means by which the illuminating beam is scanned across the sample, an image of the sample must be produced. A real image was not formed in Minsky's original design, but instead the output from the photomultiplier was translated into an image on the screen of a military surplus long persistence oscilloscope that had no provision for recording. Following the debut of his invention, Minsky later wrote that the image quality in his microscope was not very impressive because of the quality of the oscilloscope display and not because of poor resolution achieved by the microscope itself. It is now clear that the technology was not available to Minsky in 1955 to fully demonstrate the potential of the confocal approach. He stated that this is possibly a reason that confocal microscopy was not immediately embraced by the scientific community. In today's confocal microscopes, the image is serially built up from the output of a photomultiplier tube or captured using a digital camera. Afterwards it is processed in a computer imaging system and displayed on a high-resolution

video monitor, and output on a hard copy device. The information flow in a modern confocal scanning laser microscope is sketched in Figure 2-3

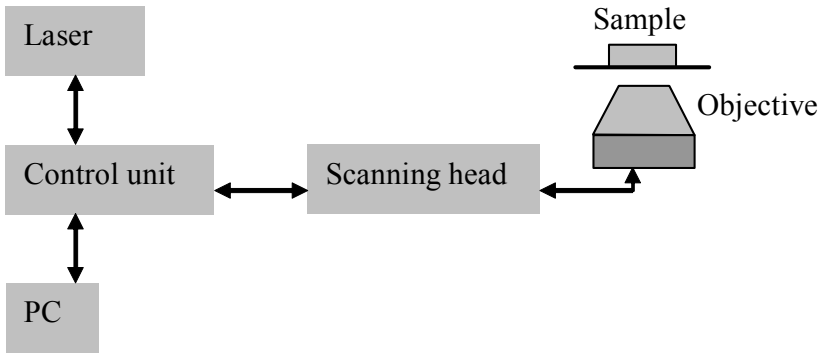

Figure 2-3 The image processing flow for CSLM

In Figure 2-4 a particular CSLM configuration, used for performing experiments reported in this thesis, is shown.

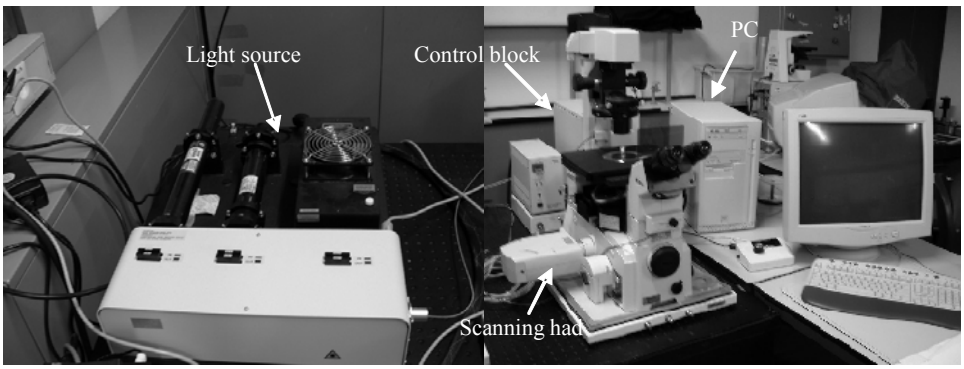

Figure 2-4 A CSLM system used for obtaining data results, reported in this thesis

References

[1]. M. Minsky, Memoir on inventing the Confocal Scanning Microscope, Scanning 10, 128-138 (1988).
[2]. T.Wilson, Confocal Microscopy, Academic Press,London,(1990).
[3]. G.E.Gervasoni et al, Cancer Research, 51, 4955-4963, (1991).
[4]. M.H.Fox et al, J. Cell Sci., 99-2, 247-253, (1991).
[5]. J.B.Powley, Handbook of Biological Confocal Microscopy, Plenum Press, NY,2-nd edition, (1995).
[6]. H.Yoshida et al, Phys. Rev. B, 44,435, (1991).
[7]. A.van Blaaderen and A. Vrij, Langmuir, 8, 2921, (1992).
[8]. A.van Blaaderen and P.Wiltzius, Science, 270, 1177, (1995).
[9]. W.K. Kegel and A. van Blaaderen, Science. 287 290, (2000).
[10]. N. B. Simeonova and W. K. Kegel, Phys. Rev. Lett. 93,035701 (2004).
[11]. N. Simeonova and W.K. Kegel, Faraday Discuss. 123 27, (2003)

3

Real-Space Fluorescence Recovery after Photo-bleaching of concentrated suspensions of hard colloidal spheres

Abstract

In concentrated suspensions of fluorescent colloidal hard spheres (close to and above the glass transition density), a part of the system is bleached in cube shaped regions using high intensity laser light. Recovery of these bleached cubes was followed in real space using confocal scanning laser microscopy (CSLM). This method provides mean squared particle displacements up to time scales that are three orders of magnitude beyond those available by present experimental techniques. It is shown that, above the (hard sphere) glass transition density, particles move over distances on the order of their own diameter on time scales of 10^6 to 10^8 Brownian times. Moreover, the mean squared displacement, $<x^2>$, shows power-law behavior over seven time (τ) decades: $<x^2> \propto \tau^{\wedge}$ (0.30±0.05). This behavior is different from earlier observations by dynamic light scattering. It is argued that these differences are caused by gravity effects, as the only difference between the systems is the buoyant mass of the colloids.

3.1 Introduction

As it was mentioned in Chapter 1, colloidal hard spheres are extensively studied experimental model systems that exhibit two fundamental transitions. The first is a thermodynamic (first-order) phase transition from a fluid to a (fcc) crystal upon increasing the volume fraction, Φ, of the spheres [1, 2, 3]. This freezing transition takes place at Φ =0.494. In between Φ =0.494 and 0.545, fluid and crystal coexist, and at higher densities a single-phase crystal is stable. The second transition occurs when a colloidal hard sphere fluid is rapidly quenched (by centrifugation, for example) to densities above approximately Φ =0.575: in that case the system is a colloidal glass [3]. This is where large-scale particle diffusion and crystallization by homogeneous nucleation stop, at least under normal gravity conditions [4]. Note, that this volume fraction is well below the volume fraction Φ =0.64, corresponding to random close packing for hard spheres. The nature of this glass transition is still in dispute. For example, the experimentally observed slowing down of particle diffusion at increasing volume fraction above the melting transition, and the arrest of structural relaxation (on experimental time scales) at the glass transition, can be described very well by Mode Coupling Theory (MCT) [5, 6]. It has recently been observed, however, that dense colloidal fluids contain distinct regions where particles move cooperatively, so-called dynamical heterogeneities [7, 8]. These heterogeneities were also found in molecular systems, both experimentally [9], and by computer simulation [10]. Dynamical heterogeneity causes a non-Gaussian distribution of particle displacements, the magnitude of which is being underestimated by MCT. Moreover, a few years ago, the notion that homogeneous nucleation stops in colloidal glasses was challenged: observations under micro gravity showed rapid crystallization of samples with high volume fractions which fail to crystallize even after a year on earth [11].

In this chapter the following two questions are addressed:

The first one is: how far do particles, on average, move in a colloidal glass?

The fundamental time scale in colloidal systems is the Brownian time, τ_B, defined as the time it takes for an infinitely diluted particle to diffuse over its own radius, i.e.,

$$t_B = \frac{r^2}{6D_0}, \tag{3.1}$$

where r is the particle radius, D_0 is the diffusion coefficient at infinite dilution being on the order of 10^{-13} – 10^{-12} m^2/s, depending on the solvent viscosity.

In concentrated systems, the mean squared displacement, $\langle x^2 \rangle$, of the particles as a function of time, τ, can be distinguished into three regimes. At small times (but already at Brownian time scales) where virtually no interparticle collisions have occurred, diffusive behavior is observed, i.e., $\langle x^2 \rangle = 6D_s\tau$, where D_s is the short-time diffusion coefficient. At intermediate times, particles are caged by their neighbors and $\langle x^2 \rangle$ as a function of time reaches a plateau: $\langle x^2 \rangle$ is almost constant as a function of time. At long times, particles have escaped these cages and again behave diffusively, i.e., $\langle x^2 \rangle = 6D_L\tau$, but now the proportionality factor between mean squared displacement and time contains the long-time diffusion coefficient, D_L (see Figure 3-1).

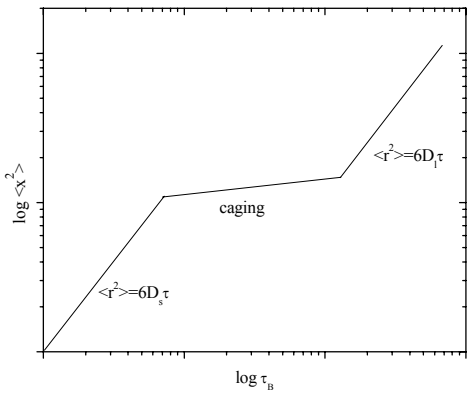

Figure 3-1 A schematic presentation of Mean Square Particle Displacement, $\langle x^2 \rangle$, in concentrated colloidal suspensions, as function of time.

At densities above the glass transition, systems apparently do not reach this long-time regime, at least not on experimental timescales. On the other hand, the 'plateaus' that are being observed above the glass transition density are not entirely flat: $\langle x^2 \rangle$ keeps increasing with time (albeit slower than linear) up to at least order 10^5 Brownian times. As the formation of a critical crystal nucleus is expected to require rearrangements of particles over roughly their own diameter, the question is simply: do they get that far? At

least after 10^5 Brownian timescales, and just above the glass transition density (Φ=0.59), particles have only moved about half their radius, as can be inferred from ref. [12]. So in principle (Brownian) time scales that are at least several orders of magnitude longer than in [12] are required to answer the question as to how far, as a function of time, colloids move in a glass. Here it will be shown that over time intervals of order 10^6-10^8 Brownian times, particles move over distances comparable to their own diameter.

The second question is: if the relation between $<x^2>$ and τ is not strictly constant, then what is it?

In other words: if a 'glass' is defined as a quenched liquid where long-time self diffusion is no longer observed, then, for hard spheres, there are two possibilities. The first is that, analogous to molecular systems, the glass transition corresponds to stretching of timescales beyond an experimental time window [13]. The second possibility is that it is a transition that couples to a principally different (relaxation) behavior. In the first scenario, long time diffusion would eventually be recovered, albeit at times that may be beyond experimental observation times. In the second case, long-time behavior would be principally different from diffusive ('diffusive' being defined as $< x^2 > \propto \tau$). A dramatic example is a system of hard spheres that is quenched to random close packing: in that case each sphere is caged by its neighbors, and $<x^2>(\tau)$ remains essentially flat. This, in fact, is the ultimate MCT scenario: a dynamic singularity.

In order to answer these questions, very long times need to be reached. 'Classical' experimental techniques are inappropriate. For example, the largest time window that can currently be reached using Dynamic Light Scattering (DLS) is several hours, due to the limited coherence time of lasers. For particles with radius R of order 0.1 μm, this corresponds to Brownian time scales of order 10^5. Tracking individual particles by confocal microscopy is limited by the fact that particles 'escape' the sampling volume and by hard disk capacity. In practice only much narrower time windows are available using this technique in comparison with DLS.

In this work the reached time scales are three orders of magnitude beyond those available by DLS. Fluorescent colloidal (hard sphere) particles are irreversibly bleached in a well defined pattern, and the sample is imaged using Confocal Scanning Laser Microscopy. Subsequently the fluorescent intensity profiles of the bleached pattern are analyzed at different times after bleaching. The detailed experimental setup is presented in the experimental section. The method is similar in principle to 'Confocal Fluorescence

Recovery After Photo-bleaching' [14] and allows determination of the mean square displacements of the particles (particles self diffusion) $< x^2 >= \int x^2 G_s(t)dx = 2Dt$, where G_s. is the self-van Hove correlation function.This method is used in the biophysics field to determine diffusion coefficients of (diluted) proteins, see, e.g., [15]. The procedure is analogous to hole burning studies (see, e.g., [16]) and 'classical' Fluorescence Recovery After Photo-bleaching (FRAP; see, e.g., [17]), but in real space. It should be noted that 'classical' FRAP suffers from similar limitations as DLS.

3.2 System and instrumental setup

The model system that is used were NBD (4-methylaminoethylmethacrylate-7-nitrobenzo-2-oxa-1,3-diazol) labeled Polymethylmethacrylate (PMMA) particles stabilized with poly(12-hydroxystearic acid) where the fluorescent dye was incorporated during the polymerization reaction with the method described in [18]. The diameter of the particles is 448 nm and their polydispersity is 5%. The particles were dispersed in a mixture of cis-decalin, tetralin and carbon tetrachloride with volume ratios 31.5 : 36.0 : 32.5 as in ref. [19]. In this mixture, particles behave as hard spheres and are almost density- and refractive index matched. They bleach rapidly at maximum laser intensity (2 mW, λ=488 nm) but only slowly at the reduced (about 10-15% of the maximum) intensity that was used for scanning the images for analysis. The size of the particles was chosen small enough so that sufficiently long time scales are accessible (note that Brownian time scales as $\tau_B \propto R^3$ with R the particle radius, see eq.(3.1)) but large enough so that translation (on average – see later) of the particles over fractions of their sizes can be followed. Due to the relatively large polydispersity, crystallization at $\Phi \geq 0.5$ is expected to be slow, in particular for dense systems with $\Phi > 0.57$. Indeed, in the most concentrated system that we studied ($\Phi = 0.59$), crystalline regions could not be observed, even after several weeks.

Using a Confocal Scanning Laser Microscope (CSLM) (see Figure 2-4), profiles were bleached in the form of (3 dimensional) cubes with linear sizes on the order of 10 to 100 particle diameters in the focal plane, and order 10 diameters in thickness. Subsequently the systems were imaged, also by CSLM, by scanning several slices perpendicular to the field of gravity, at different times (from minutes to several weeks). The sample cell that was used is shown in Figure3-2.

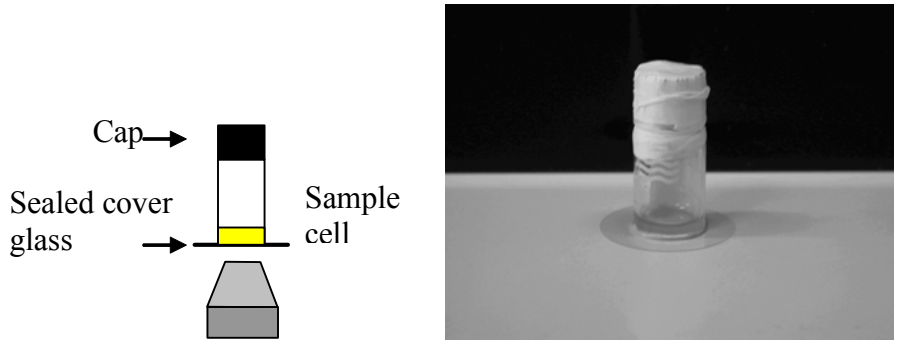

Figure 3-2 Experimental sample cell.

3.3 Data analysis

Profiles were obtained by integrating the fluorescent intensities along both perpendicular directions of the slices (perpendicular to a side of the cube), resulting in four intensity profiles. These were compared in order to check if flow occurred, averaged, and normalized with respect to the fluorescent intensity far away from the bleached cube. Averages were taken over several slices. As it was mentioned in the introduction to this chapter, the method of fluorescent recovery after bleaching in concentrated colloidal systems, allows measurement of the mean square particle displacements.

The probability of finding a (fluorescent) particle at position x on a line at time, τ, provided that its initial position is x_0, is the canonically averaged displacement distribution (the self-van Hove correlation function) given by

$$p(x, x_0, \tau) = \sqrt{\frac{1}{4\pi D\tau}} \exp\left(\frac{-(x - x_0)^2}{4D\tau} \right) \tag{3.2}$$

where D is the diffusion coefficient. Although this Gaussian form is not strictly correct for concentrated systems (in particular close to the glass transition), deviations from Gaussian behavior tend to disappear on the long timescales that are studied (see [7, 8, 23, 24]), although they may persist for long times in certain glassy states [25].

Two half spaces are considered. One of them, extending from x=0 to ∞, contains the bleached part of the sample. The other one, extending from x=-∞ to 0, is the unbleached part, consisting of fluorescent particles. This is the (ideal – see below) situation directly following the bleaching process (see

Figure 3-3), assuming that this process is fast compared to the relaxation times (time needed for the particle system to reach equilibrium) of the particles, and that the width of the laser beam is small compared to the particle size. Then, the probability of finding a fluorescent particle at position x after a certain time, τ, independent of it's original position x_0 is

$$p(x,\tau) = \int_{-\infty}^{0} p(x, x_0, \tau) dx_0 = \frac{1}{2}(1 - erf\left(\frac{x}{2\sqrt{D\tau}}\right)) \tag{3.3}$$

In this equation, $erf(z) = \frac{2}{\sqrt{\pi}} \int_0^z e^{-t^2} dt$ is referred to as the error function. Eq. (3.3) is just the time development of the integrated (normalized) fluorescent intensity profile $I(x, \tau)$ along one of the two axes perpendicular to the sides of the cube, i.e.,

$$I(x,\tau) = \frac{I}{I_\infty} \int_{cube-side} (x, y, \tau) dy = p(x,\tau) \tag{3.4}$$

or

$$I(x) = \frac{1}{2}(1 - erf\left(\frac{x}{2\sqrt{D\tau}}\right)) \ , \tag{3.5}$$

where the assignments x and y are arbitrary as long as they are perpendicular to one another and to a side of the cube. This equation implies that the initial intensity profile (at τ=0) is a step function at $x=0$ with $I(x \leq 0)$=1 and $I(x \geq 0)$=0. In practice, this is not the case. Instrumental properties cause significant deviations from this 'ideal' initial profile. Probably the most important one is a finite width of the laser beam, which (for clarity reasons) has been neglected in the derivation. As the intensity profile of the laser beam is, to a good approximation, Gaussian, it can be deduced from the derivation that the initial profile is expected to have the same form as eq.(3.5), with $D\tau$ replaced by a quantity that is related to the width of the laser beam. In Figure 3-3 is shown a bleached cube in a system that is randomly close packed (Φ=0.64) and where particles cannot move. Its intensity profile is shown also in Figure 3-3. It reflects the 'instrumental' contribution and is indeed quite well described by eq.(3.5), as can be seen in the figure. This measured profile is quantitatively reproduced even weeks later, and also is indistinguishable from a profile that was bleached in a system with Φ=0.59 and measured after

less than a minute. These observations indicate that the time development of the profile can only be caused by particles moving in and out of the bleached region.

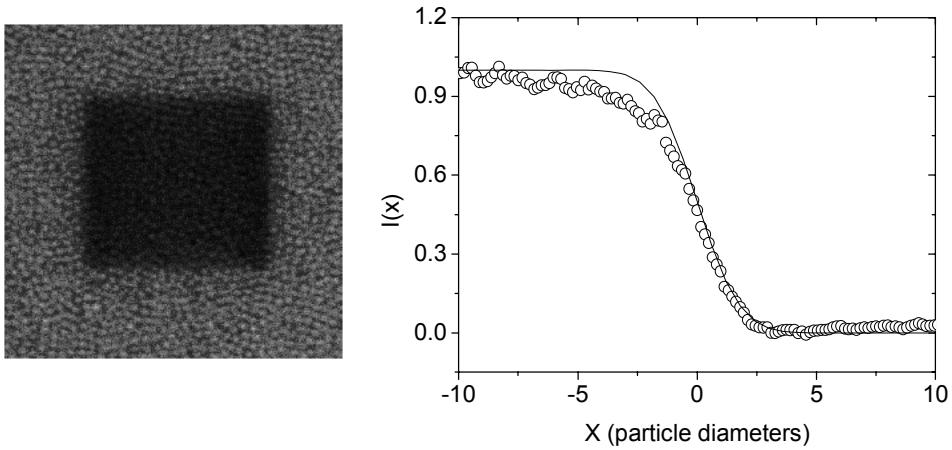

Figure 3-3 Left- Bleached cube in a randomly close packed hard sphere suspension with volume fraction Φ=0.64. The size of the cube in the focal plane is 11 μm (25 particle diameters). As only a thin slice (of 3-5 particle diameters) was bleached, some fluorescence is still apparent in the bleached part of the sample. The fluorescence in this region comes from particles that are out of the focal plane. Right - Normalized (horizontal) intensity profile representing the left part of the system (in fact the profile is averaged over all sides of the cube). The line is eq. (6) with b=0.8 particle diameters.

Clearly, the part of the intensity profile where $x<0$ is more curved than described by eq.(3.5). This is probably due to scattering of the laser light by the particles, causing additional bleaching. This effect is not detectable for $x>0$ and is neglected in the analysis. The data are fitted to

$$I(x) = \frac{1}{2}(1 - erf\left(\frac{x}{2\sqrt{b}}\right)) \quad , \tag{3.6}$$

where b is simply related to the half width of the laser beam (if the half width is σ then $b = \sigma\sqrt{2}$. The profiles for systems with Φ<0.64 are then described by

$$I(x) = \frac{1}{2}(1 - erf\left(\frac{x}{2\sqrt{D\tau + b}}\right)) \tag{3.7}$$

The profile has some interesting properties:

(1). Its 'zeroth moment' in positive half space is proportional to the square root of time, i.e.,

$$A(\tau) = \int_0^\infty I(x,\tau)dx = \sqrt{\frac{D\tau}{\pi}} \tag{3.8}$$

(2). But any value of x where $I(x, \tau)$ is some fraction of its value at x=0 is also proportional to the square root of time. In this work the value of x where the intensity is half the intensity at x=0 is used. This value of x is $x_{1/2}$, given by

$$\tfrac{1}{2} I(x = 0, \tau) = \frac{1}{4} = \frac{1}{2}(1 - erf\left(\frac{x_{1/2}}{2\sqrt{D\tau}}\right)) \tag{3.9}$$

In equations 3.8 and 3.9 $b=0$ for convenience.
The intensity $I(x, \tau)$ is normalized with respect to the fluorescent intensity far away from the bleached cube I_∞ in eq.(3.4). In the coordinate system defined above, the profile goes from 1 (at negative values of x) to 0 (at positive values of x) and equals ½ at x=0 (we make use of this property in eq.(3.9)), (see Figures 3-3 and 3-4). This is always true if the bleached and unbleached volumes are equal. In general, it is a (very) good approximation if only a small fraction of the cube is recovered by fluorescent particles, as is the case in this work

Solving numerically the equation $erf\left(\frac{x_{1/2}}{2\sqrt{D\tau}}\right) = \frac{1}{2}$ leads to

$$x_{1/2} \approx 0.954\sqrt{D\tau} \tag{3.10}$$

This result can immediately be compared to the important result that the second moment of the (Gaussian) displacement distribution, eq.(3.2) with x_0=0, is

$$< x^2 >= 2D\tau \tag{3.11}$$

so that

$$x_{1/2}^2 \approx 0.455 < x^2 > \tag{3.12}$$

The values of x where the fluorescent intensity is half the intensity at x=0, $x_{1/2}$, were corrected by subtracting the value of $x_{1/2}$ determined for the system with Φ=0.64

Eq.(3.12) provides the link between earlier results arising from Dynamic Light Scattering (DLS) [12], microscopy [7, 8, 23] and computer simulation.

The numerical factors in eqs.(3.10) and (3.12) correspond to a Gaussian displacement distribution (eq. (3.2)). Any deviation from Gaussian behavior leads to a different time dependence of the displacements, eq.(3.10) and eq.(3.11). Such deviations will show up if the values of $x_{1/2}$ are compared to the values of $D\tau$ that result from fitting eq.(3.3) to the experimental intensity profiles.

3.4 Results and discussion

In Figures 3-4(A) and 3-4(B), CSLM images are shown of cube shaped patterns at different times after bleaching, for two volume fractions, Φ=0.45 and Φ=0.59. The Brownian time is τ_B=0.0263 s in this system.

It can immediately be seen from these images that fluorescent particles move deeper into the bleached cubes as time proceeds, the process being much faster for the system with smallest volume fraction. This effect is quantitatively shown in Figures 3-4(C) and 3-4(D), where the normalized intensity profiles are plotted together with the theoretical profiles, eq.(3.7). Clearly, at x>0 the profiles are quantitatively described by eq.(3.7) for all times, even very long ones. This is not the case for the profiles at x<0, probably as a result of scattering (as discussed in the previous section). However, this does not affect the analysis. In particular for the system with Φ=0.59 (see Figure 3-4(D)), data are quite noisy. The reason is that much smaller cubes (linear size 11 μm) were analyzed compared to the system with Φ=0.45 (linear size 65 μm), resulting in a higher resolution but more noise because of (effectively) smaller numbers of particles being averaged over.

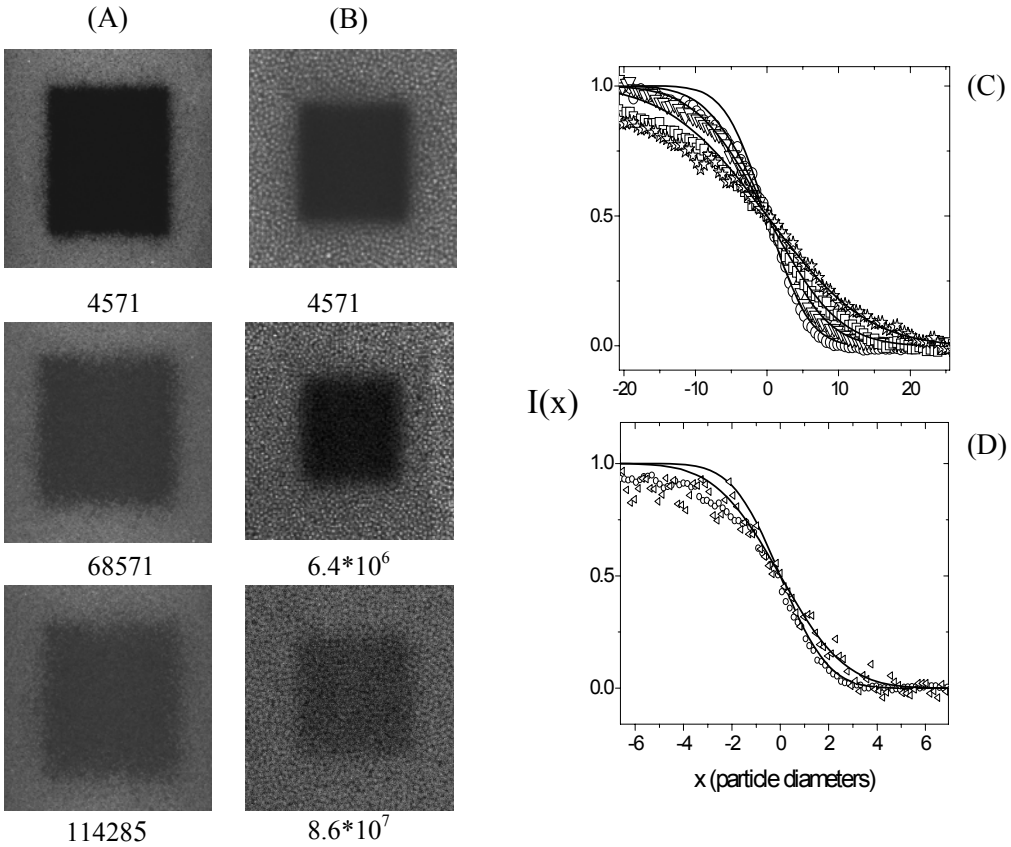

Figure 3-4 (A) Bleached cubes in a colloidal hard sphere suspension with volume fraction Φ=0.45 at different times: 4571, 68571 and 114285 Brownian time units (indicated in the figure) where the Brownian time is τ_B=0.0263s for the definition see eq.(3.1). The sizes of the bleached cubes in the focal plane are 65 μm (145 particle diameters) and their thicknesses are 3.2 μm.

(B) Same as fig. 3-4(A), but now for a system with Φ=0.59 at a Brownian times of 4571, 6.4*10^6, and 8.6*10^7. The dimensions of the cubes are 11 μm in the focal plane and a thickness of 5.08 μm.

(C) Normalized fluorescence intensity profiles, I(x), of the cubes shown in fig.3-4 (A). The points correspond to 4571 (circles), 32000 (triangles), 68571 (diamonds) and 114285 (stars) Brownian times units. Corresponding lines are eq.(3.4) with $2\sqrt{D\tau + b}$ =6.5, 9, 11, and 15.5 particle diameters. By subtracting the average intensity around the center of the cubes, data are corrected for fluorescent particles moving in from outside the cubes in the vertical direction. Averages were taken over 5 to 6 slices in a cube.

(D) Same as fig.3-4(C), but now for the system with Φ=0.59 shown in fig. 3-4(B). Circles and triangles are the normalized intensity profiles taken 4571 and 6.4*10^6 Brownian time units after bleaching, respectively. Lines are eq.(3.7) with $2\sqrt{D\tau + b}$ =2.2 and 3 particle diameters. Averages were taken over 7 to 9 slices in a cube.

The values of the (long time) diffusion coefficient, D, can be extracted from the values of $x_{1/2}$ that follow directly from the profiles in Figures 3-4(C) and 3-4(D). These values vary in between 0.005 and 0.015 (in units of D_0) for Φ=0.45 which is compatible with the value 0.018 for Φ=0.466 as reported in [12] but the error range is large. The values of D for the system with Φ=0.59 are on the order of 10^{-8}, but this value cannot be interpreted as a long-time diffusion coefficient, as it is shown in Figure 3-5 that long-time diffusion (i.e., $\langle x^2 \rangle \propto \tau$) is not observed for this system.

In Figure 3-5 the values of $x_{1/2}^2 / 0.455$ are plotted (the dividing factor being chosen so that direct comparison with $\langle x^2 \rangle$ is allowed, see eq.(3.12)) as a function of time for the systems with volume fractions Φ=0.45 and 0.59. For comparison, values of $\langle x^2 \rangle$ are plotted, obtained from analyzing displacements of individual particles, as reported in [7], in the same figure. Although this method also makes use of CSLM, it is a principally different method from the one that is employed in this work. The values of $\langle x^2 \rangle$ *(=*$\langle r^2 \rangle$*/3)* (with $\langle r^2 \rangle$- displacements in 3D), that were reported by van Megen and coworkers [12] and obtained by Dynamic Light Scattering (DLS) are also plotted.

It can be seen in Figure 3-5 that the data obtained in this work and those from [7] can simply be connected by straight lines in the log-log representation. This is to be expected for the system with Φ=0.45: from approximately 10 Brownian time units on, this system is in the long-time diffusion limit (see the introduction), being characterized by a unit slope in Figure 3-5. The (two) points at earlier times clearly correspond to the intermediate regime. The short-time diffusion regime cannot be sampled by CSLM technique because of the finite scanning speed (0.25s per frame). This regime is obvious from the (DLS) data of van Megen and coworkers (up to 10^{-1} Brownian time units – note that their data at even smaller timescales are not shown). From this result can be concluded that the system with Φ=0.45, at long times, behaves as expected and thus that applied new method for determining displacements 'works'. Although the data are somewhat scattered around the line of unit slope in Figure 3-5, at least the procedure results in the expected order of magnitude for the mean squared displacements (further abbreviated as MSD)

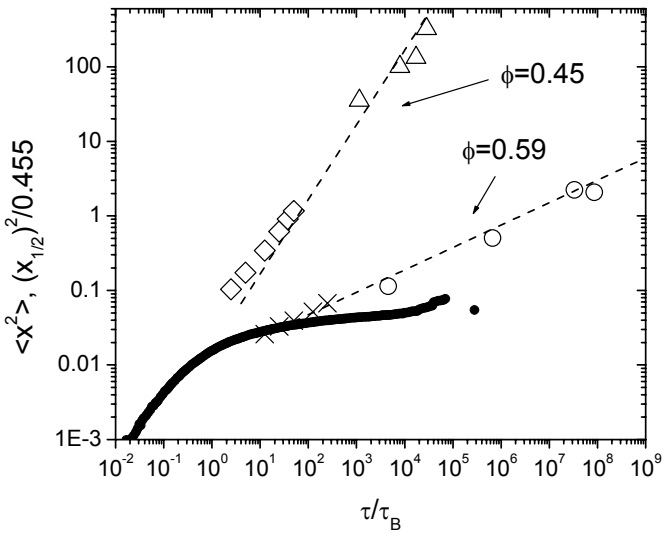

Figure 3-5 Mean squared displacements $<x^2>$ and $(x_{1/2})^2/0.455$ (as defined in the text) in units of the squared particle radius versus time in units of Brownian time τ_B. The values of $x_{1/2}$ that resulted from the profiles in figs.3-4 (C) and (D) were corrected for the 'instrumental' contribution (of magnitude 1.66 particle radii) as shown in fig.3-3. Triangles correspond to the system with volume fraction Φ=0.45 and open circles to the system with Φ=0.59. Diamonds and crosses are (CSLM) data reported in [7] obtained from tracking individual particles with Φ=0.45 and 0.60, respectively. The dense black line are data from van Megen and coworkers [12] obtained with DLS for Φ=0.59 The upper dashed line connects the two sets of data for Φ=0.45 and is given *by* $<x^2>=(x_{1/2})^2/0.455=0.0167(\tau/\tau_B)$. The lower dashed line connects the datasets for Φ=0.59 and 0.60 from this work and the work reported in [7] and is given by $<x^2>=(x_{1/2})^2/0.455=0.012(\tau/\tau_B)^{0.3}$.

For the dense system with $\Phi=0.59$, it immediately emerges from Figure 3-5 that the mean squared displacements are larger, at comparable time scales, than the ones that were reported by van Megen and coworkers [12] for a system with the same volume fraction. For example at τ/τ_B=4571, the particles move $\sqrt{< x^2 >} \approx 0.34$ particle radii, where as it follows from the data of van Megen and coworkers that they move $\sqrt{< x^2 >} \approx 0.22$ particle radii (see Figure 3-5). The data reported here are however consistent with earlier measurements (crosses in Figure 3-5), using a principally different method. The tendency of the MSD to increase with time (crosses in Figure 3-5) is extended to the much longer timescales studied here (open circles in Figure 3-5). In particular, the data are consistent with a power-law behavior: $<x^2> \propto \tau^{(0.30\pm0.05)}$ over 7 time decades, reaching displacements on the order of a particle diameter. This behavior is fundamentally different from predictions by Mode Coupling Theory. On the other hand, the DLS data from [12] in

Figure 3-5 also show a slowly increasing MSD with time, although this increase is not as steep as observed for our data, and does not follow power-law behavior.

The only difference between the systems studied by van Megen and coworkers on the one hand, and the ones studied here and in [7] on the other hand, is the buoyant mass of the colloidal particles. The mass density difference between the PMMA particles and the solvent in the mixture of tetralin and decalin in [12] is $\Delta\rho_m \approx 0.3$ g/ml, while in system used here it is roughly an order of magnitude smaller. Therefore, a possible explanation of the much steeper increase of $\langle x^2 \rangle$ found here is that the system of van Megen and coworkers is slowed down by gravity effects. The particles used in this work are of comparable size as the ones in [12], and so is the solvent viscosity. The most obvious effect of gravity is sedimentation, resulting in densification of the systems. The relative time scales, where sedimentation effects become apparent can be easily estimated. The time scale where particles sediment over a height Δh is $\Delta t = \Delta h / v_{sed} \propto 1/\Delta\rho_m$, where v_{sed} is the sedimentation velocity which is proportional to the (mass) density difference for equally sized particles. If the plateau in $\langle x^2 \rangle$ versus τ as found by van Megen and coworkers is caused by sedimentation effects (or consequences of sedimentation effects), then the above argument implies that the data reported here are supposed to undergo the same fate, with a delay of only a decade in time. Clearly, this is not what happens. The much steeper increase of the MSD with time that we find persists over many decades. Only the data point at 10^8 Brownian time units suggests 'collapse' of the system, but this needs to be verified. Therefore a conclusion can be made that (consequences of) sedimentation does not explain the difference between our data and the DLS results. Still, it is expected gravity to play a role: as mentioned in the introduction, a colloidal glass was found to crystallize rapidly under micro gravity [11], and also in a density matched solvent (with $\Delta\rho_m$ even an order of magnitude smaller than the one studied here) [20]. In the system studied here, the polydispersity of 5% in combination with a small gravitational field apparently suppresses crystallization. The influence of gravity is therefore expected to be more subtle and possibly is related to the buildup of stress in the system [21]. An intriguing question that remains is what mechanism, on particle length scales, leads to behavior of the form $\langle x^2 \rangle \propto \tau^{0.30}$? Recently it was shown that particles moving in one dimension ('file movement') results in $\langle x^2 \rangle \propto \tau^{0.5}$ see, e.g.,[22]. This behavior reflects 'single file diffusion',

which implies that the displacements of the particles are highly correlated and collective.

3.5 Conclusions

In this chapter the displacements of colloidal particles at very long (Brownian) time scales were determined: three orders of magnitude longer than the previous state of the art. Questions were addressed as to how far particles move in a colloidal hard sphere glass, and what the relation is between the mean squared displacement (MSD) and time on long timescales. It was shown that particles move over distances on the order of their own diameter on time scales on the order of 10^8 Brownian times. Moreover the MSD data are consistent with $<x^2> \propto \tau^{(0.30\pm0.05)}$ over 7 time decades. This increase is much steeper than the extrapolated behavior of MSD's measured previously by dynamic light scattering (DLS). The increase is however consistent with earlier measurements where individual particles were tracked. Gravity may be responsible for the difference between reported here MSD data and those obtained by DLS and in the next chapter results from gravity-controlled experiments are reported.

Acknowledgements

Thanks to Alfons van Blaaderen for continuing discussions and suggestions, Bill van Megen for kindly providing the DLS data, and Gijsje Koenderink for comments on the manuscript. Els de Hoog is thanked for bringing to our attention references on 'confocal FRAP' in the biophysics field.

References

[1]. Wood, W.W. and J.D. Jacobsen, J. Chem. Phys., 27, 1207, (1957).
[2]. Alder, B.J. and T.E. Wainwright, J. Chem. Phys., 27, 1208, (1957).
[3]. Pusey, P.N. and W. van Megen, Nature, 320, 340, (1986).
[4]. van Megen, W. and S.M. Underwood, Nature, 362, 616, (1993).
[5]. Gotze, W. and L. Sjogren, Phys. Rev. A, 43, 5442, (1991).
[6]. van Megen, W. and S.M. Underwood, Phys. Rev. Lett., 70, 2766, (1993).
[7]. Kegel, W.K. and A. van Blaaderen, Science, 287, 290, (2000).
[8]. Weeks, E.R., et al., Science, 287, 672, (2000).
[9]. Cicerone, M.T. and M.D. Ediger, J. Chem. Phys., 103, 5684, (1996).
[10]. Kob, W., et al., Phys. Rev. Lett., 79, 2827, (1997).
[11]. Zhu, J., et al., Nature, 387, 883, (1997).
[12]. van Megen, W., et al., Phys. Rev. E, 58, 6073, (1998).
[13]. Angell, C.A., Science, 267, 1924, (1995).

[14]. Kubitscheck, H., P. Wedekind, and R. Peters, Biophys.J., 67, 946, (1994).
[15]. Gribbon, P. and T.E. Hardingham, Biophys. J., 75, 1032, (1998).
[16]. Kircher, O., B. Schiener, and R. Böhmer, Phys.Rev.Lett., 81, 4520, (1998).
[17]. Imhof, A., et al., J. Chem. Phys., 100, 2170, (1994).
[18]. Bosma, G., et al., J. Colloid Interface Sci., 245, 292, (2002).
[19]. Hoog, E.H.A.d., et al., Phys. Rev. E, 64, 021407, (2001).
[20]. Kegel, W.K., Langmuir, 16, 939, (2000).
[21]. Liu, A.J. and S.R. Nagel, Nature, 396, 21, (1998).
[22]. Wei, Q.H., C. Bechinger, and P. Leiderer, Science, 287, 625, (2000).
[23]. Kasper, A., E. Bartch, and H. Sillescu, Langmuir, 14, 5004, (1998).
[24]. Mortensen, T.C. and W. van Megen. in Slow Dynamics in Complex Systems, Fukuoka, Japan: AIP Conference Proceedings,(1998).
[25]. Vollmayr-Lee, K., et al., J. Chem. Phys., 116, 5158, (2002).

4

Gravity-induced aging in glasses of colloidal hard spheres

Abstract

The influence of gravity on the long-time behavior of the mean squared displacement in glasses of polydisperse colloidal hard spheres was studied by means of real-space fluorescent recovery after photo bleaching. For the first time, a significant influence of gravity on the mean squared displacements of the particles is presented. In particular, the systems which are glasses under gravity (with a gravitational length on the order of tens of micrometers) show anomalous diffusion over several decades in time if the gravitational length is increased by an order of magnitude. No influence of gravity was observed in systems below the glass transition density. It is shown that this behavior is caused by gravity dramatically accelerating aging in colloidal hard sphere glasses. This behavior explains the observation that colloidal hard sphere systems which are a glass on earth rapidly crystallize in space.

4.1 Introduction

As already mentioned in the introduction to Chapter 3, hard spheres for which the potential energy is infinite on overlap and (in the absence of fields) zero otherwise, freeze upon increasing number density from a fluid into a crystal at a volume fraction, Φ, of 0.494 [1,2]. In between Φ =0.494 and 0.545, fluid and crystal coexist [3], while at even higher volume fractions, a single phase (fcc [4]) crystal is thermodynamically stable up to the close packed density corresponding to $\Phi = \pi / 3\sqrt{2} \approx 0.74$ [5]. After quenching a colloidal system, in the resulting colloidal glass, large-scale particle diffusion and crystallization by homogeneous nucleation stop, suggesting that crystal nucleation proceeds by large-scale particle diffusion [6] [7]. It is widely believed that the glass transition of hard spheres corresponds to permanent caging of the particles by their neighbors [7,9]. However, recent computer simulations [10] and experiments under microgravity [11] pose serious doubts on the very existence of a glass transition at Φ <0.64 of monodisperse hard spheres in the absence of a gravity field. These studies show that monodisperse [10] but also (about 5%) polydisperse [11] hard spheres crystallize in the absence of gravity up to volume fractions close to 0.64. In the last study, a system that is a glass on earth rapidly crystallizes in space after homogenization by mixing.

While microscopic particle movements do not seem to be affected by details of the particle size distribution [12], no quantitative studies of the influence of gravity on dynamics in concentrated colloidal suspensions have been reported. In this chapter the question as to what the influence of gravity is on particle mobility (quantified by the mean squared displacement) in glassy systems is addressed. For this purpose, here is used a polydisperse (7%) system in order to suppress crystallization, at least on experimental time scales. By this construction, crystallization and its consequences (e.g., Ostwald ripening at very long time scales) will not interfere with the (global) particle dynamics.

4.2 Experimental section

Systems with two different gravitational lengths are studied in this chapter. One is of order of 0.1 millimeter (referred to as low gravity) and

second one of order of 10 micrometer (normal gravity – "normal" refers to the situation for most colloidal model systems, at least for the ones with comparable sizes as studied here). The gravitational length is defined by $h = kT/(\frac{4\pi}{3} R^3 \Delta\rho g)$, where k is Boltzmann's constant, T is the temperature, R is the particle radius, g is the acceleration due to gravity and $\Delta\rho$ is the mass density difference between the particles and the solvent. The mass density of the solvent is adjusted so as to vary the gravitational length.

For all experiments, again is employed fluorescent labeled system of NBD (4-methylaminoethylmethacrylate-7-nitrobenzo-2-oxa-1,3-diazol) labeled polymethylmethacrylate (PMMA) particles. Their synthesis is described in details in [13]. The average radius of the particles is 295 nm and their polydispersity is 7%. The particles were dispersed in two different mixtures corresponding to the two different gravitational conditions referred to above. The first is a density-matched mixture of cis-decalin, tetralin and carbon tetrachloride with volume ratios 31.5 : 36.0 : 32.5, where $\Delta\rho$=0.02 g/ml, so that h=0.2mm for R=295nm. Better matching (smaller $\Delta\rho$) is possible [14], but in that case the particles bleach too quickly for the present purpose. The second solvent that is used is a mixture of cis-decalin and tetralin with volume ratios 68.0 : 32.0. In these systems $\Delta\rho$=0.3 g/ml so that h=13μm. Note, that microgravity experiments in space correspond to gravitational lengths, h, on the order of meters.

As shown in refs. [15] and [16] for the first situation, and in [6] for the second, in these solvent mixtures particles behave as hard spheres and are refractive index matched. Some density matching solvents are notorious for causing charge on the particles, see, e.g., [17,18]. However, in the solvent mixture employed here, no indications for the presence of charge have been observed [16,15]. Therefore, the only difference between the low gravity and the normal gravity system is the gravitational length.

In principle, the self-intermediate scattering function, being the Fourier transform of the mean squared displacement, can be measured by dynamic light scattering (DLS), see, e.g., [19]. However, due to the limited coherence time of lasers, only time scales on the order of hours can be reached by this technique. In order to reach longer time scales, which is necessary for the kind of concentrated systems of interest, real-space fluorescent recovery after photo bleaching (FRAP) is applied as recently developed method for colloidal systems and reported in [20]. This method makes use of Confocal Scanning Laser Microscopy (CSLM), and allows

following particles over time windows that are up to three orders of magnitude longer than those reached by DLS.

The method is described in detail in Chapter 3, and will only be summarized here. Using a CSLM, profiles were bleached in the form of cubes with linear sizes on the order of 10 to 100 particle diameters in the focal plane, and order 10 diameters in thickness. Subsequently the systems were imaged, also by CSLM, by scanning several slices perpendicular to the field of gravity, at different times (from minutes to several weeks). By integrating the fluorescent intensities along the sides of the bleached cubes, intensity profiles were obtained. The decay length of the fluorescent intensity profile, defined by the length where the intensity is half the (normalized) intensity of the unbleached part of the sample, $x_{1/2}$, is related to the mean squared displacement $<x^2>$ by

$$< x^2 > \approx 2.20 x_{1/2}^2 \tag{4.1}$$

4.3 Results and discussions

All data presented in the subsequent Figures are averaged over 4 to 8 cubes per volume fraction, the standard deviation being on the order of 10%. The displacements are in units of the particle radius, and time is in units of the Brownian time $\tau_B = R^2/6D_0 \approx 0.059$s for this particular system, where D_0 is the diffusion coefficient at infinite dilution. The size of the particles was chosen small enough so that sufficiently long time windows are accessible and large enough so that translation (on average) of the particles over fractions of their sizes can be followed.

In Figures 4-1(A) and 4-1(B) the mean squared displacements in samples under the two gravity conditions referred to above: low gravity (Figure 4-1(A)) and normal gravity (Figure 4-1(B)), are shown. Clearly, there is no significant difference between low gravity and normal gravity conditions below volume fractions of 0.55. These suspensions show typical diffusive behavior, characterized by a unit slope in the Figures, i.e., $<x^2> \propto \tau$. However, there is a dramatic influence of gravity on samples with higher volume fractions. From Figure 4-1(A) it is clear that particles under low gravity move on average over distances on the order of a particle diameter in 10^7-10^8 Brownian time units, and they seem to obey a power law given by

$\langle x^2 \rangle \propto \tau^{0.3}$ over more than 5 decades in time. In contrast, particles under normal gravity only move over distances that are an order of magnitude smaller - they reach a plateau region after roughly 10^4-10^5 Brownian time units and thus remain a true "glass" within the experimental time window.

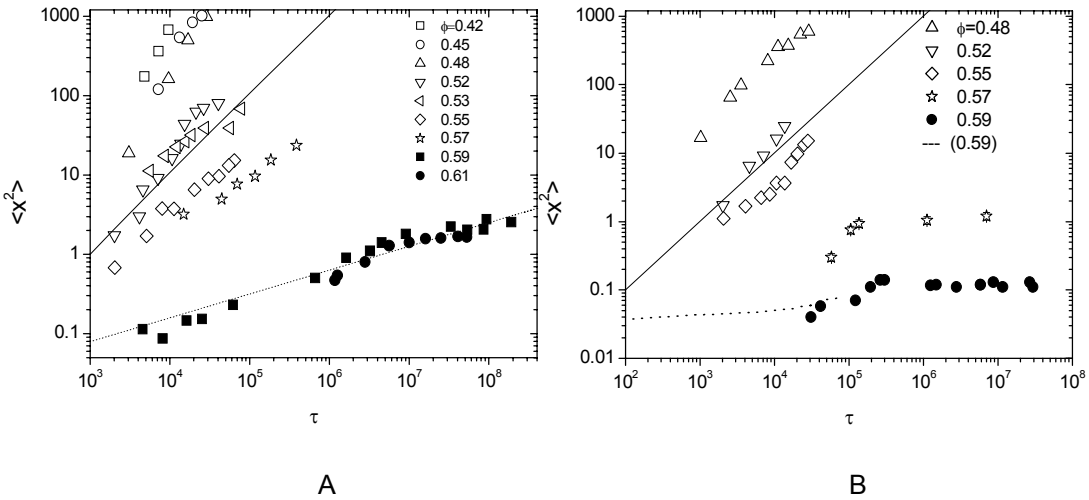

Figure 4-1 Mean squared displacements $\langle x^2 \rangle$ (as defined by eq.(4.1) in the text) in units of the squared particle radius versus time, τ, in units of Brownian time τ_B (for a definition see text).(A)Particles under low gravity (in a density matched solvent). The solid line with unit slope has been drawn to indicate diffusive behavior. The dotted line is given by $\langle x^2 \rangle = 0.012\tau^{0.3}$. The volume fractions of the systems are indicated in the Figure. Open symbols correspond to volume fractions below the glass transition volume fraction of 0.58, and filled symbols are for the volume fractions above the glass transition. (B) As (A) but now for systems under normal gravity. In this Figure the dotted line are data from van Megen [19], to be compared to our data for a volume fraction of 0.59.

In the same Figure 4-1(B) the DLS data from van Megen [19] are plotted. These data, clearly, are consistent with the new data under normal gravity conditions. Obtained results indicate a strong influence of gravity on particle displacements. This is surprising, as the gravitational length in the system, even under normal gravity (where h=13μm), equals many particle diameters. Thus, it must be that gravity couples to movements involving many particles, such as shear inhomogeneities [7] or dynamical heterogeneities [16,21]. The question that emerges is: what is the influence of the gravity on the aging behavior of colloidal glasses? Earlier studies indicate that glassy systems of colloidal hard spheres under gravity age [19], i.e., the function $\langle x^2 \rangle(\tau)$ depends on the waiting time. The waiting time is defined as the time (after homogenization) the suspension is left undisturbed before starting the experiments.

The mean squared displacements after several waiting times, $t_{w,}$ were measured. In Figure 4-2 the results for a system under normal gravity and with a volume fraction of 0.59 are presented. t_w =0 corresponds to starting the measurements immediately after the sample was prepared. The other data in the figure correspond to waiting times of 1 to 5 days, indicated in the Figure. It can be seen in Figure 4-2 that in a window of 5 days, there is a weak slowing-down of particle movements upon increasing waiting time. These observations are comparable to those reported in ref. [19], and might well be caused by sedimentation of the particles. As can be seen in Figures 4-3(A) and 4-3(B), the situation is completely different for the glassy systems under low gravity: the systems gradually move over smaller and smaller distances the longer the waiting time. After t_w=12-17 days, the mean squared displacements in the systems under low gravity are comparable to those for the systems under normal gravity conditions, but with t_w=0. These observations indicate that gravity significantly accelerates aging in colloidal glasses: low gravity systems reach "the state of normal gravity systems" only after many (order 10^7 in this case) Brownian time units following homogenization of the system. The observations in Figure 4-2 imply that at very long times, say $\tau>10^7$, $<x^2>$ should reach a plateau even for t_w=0. The data for Φ >0.57 in Figure 4-1(A) (and t_w=0 in Figures 4-3(A) and 4-3(B)) are not inconsistent with that. However, sufficient data available beyond $\tau=10^7$ were not obtained, to be able to unambiguously determine the functional form of $<x^2>(\tau)$. Therefore the data for $t_w>0$ in Figure 4-3(A) are rescaled to t_w=0. In rescaling, the new values of τ are given by $\tau^* = (\tau + t_w)$ and the new values of $<x^2>$ by $<x^2>^*(\tau^*) = [<x^2>(t_w=0, \tau= t_w) + <x^2>(t_w, \tau)]$. The result is shown in Figure 4-4. This Figure unambiguously shows a plateau of $<x^2>$ for $\tau>10^7$ Brownian time units. A conclusion can be made that the power law behavior observed here (see also ref. [20]) corresponds to transient behavior in the systems studied. It is an interesting open question whether the plateau as in Figure 4-4 will ever be reached in even weaker gravity fields, such as microgravity.

It is tempting to speculate that relaxation of shear inhomogeneities, which will always form upon preparing colloidal systems with high volume

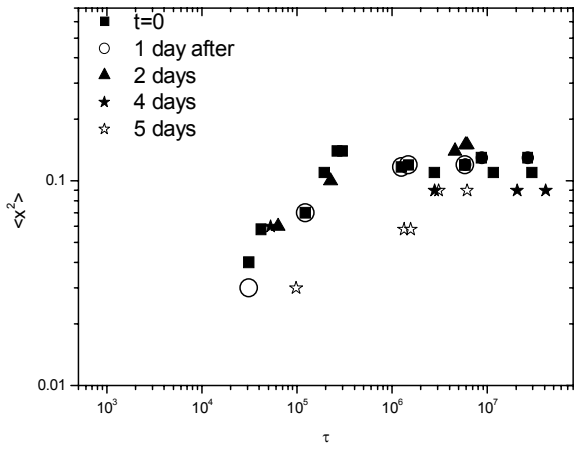

Figure 4-2 Mean squared displacement of a system under normal gravity after several waiting times, t_w as indicated in the Figure. The volume fraction of the colloids is 0.59.

fractions, is responsible for the dramatic influence of gravity on the aging behavior that is observed. If it is, then, in principle, the behavior of the systems should depend on the way they are prepared (that is, homogenized). So far there were no indications for that being the case.

Independent of the mechanism causing the aging behavior, the results qualitatively explain why it is that systems that are glasses on earth rapidly crystallize in space, as observed in [11]. In order for crystals to form, it is expected that the time to form crystal nuclei (say, roughly, 1/(nucleation rate)) should be within the time window that particles move over distances on the order of their own diameter. In that case a significant number of particle cages will have broken down, enabling particles to rearrange and form crystal nuclei. This can be accomplished under low gravity (and apparently microgravity [11]), but not under normal gravity, as clearly shown by comparing Figures4-1(A) and 4-1(B).

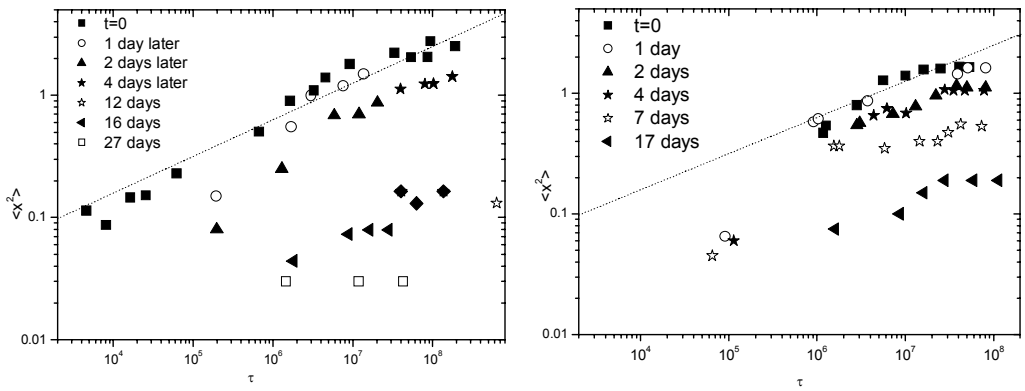

A B

Figure 4-3 As Fig.4-2, but now under low gravity. The volume fractions are 0.59 (A) and 0.61 (B). The dotted lines are given by $\langle x^2\rangle = 0.012\tau^{0.3}$.

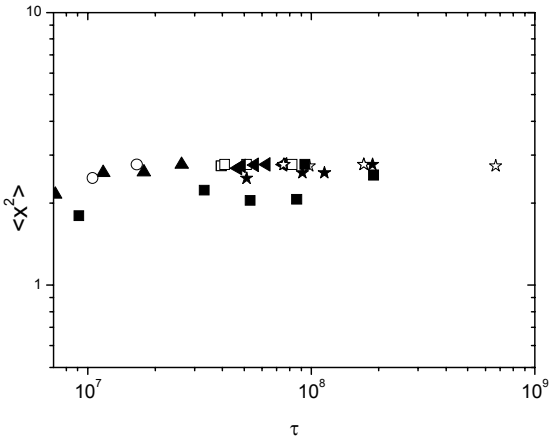

Figure 4-4 Rescaled values of the mean squared displacements from Fig.4-3(A). In rescaling, the new values of τ are given by $\tau^* = (\tau + t_w)$ and the new values of $\langle x^2\rangle$ by $\langle x^2\rangle^*(\tau^*) = [\langle x^2\rangle(t_w=0, \tau) + \langle x^2\rangle(t_w, \tau)]$.

4.4 Conclusions

A quantitative influence of gravity on particle mobility in glassy colloidal systems was shown for the first time. Gravity dramatically accelerates aging in glassy systems, thereby reducing the time window in

which crystal nucleation may proceed, which lowers the glass transition density. The important question that remains is by what precise mechanism gravity couples to (collective) particle movements.

Acknowledgements

Thanks to Bill van Megen for kindly providing his data, and Dirk Aarts and Roel Dullens for comments on the chapter.

References

[1]. W.W. Wood and J.D. Jacobsen, J.Chem.Phys., 27, 1207, (1957)
[2]. B.J. Alder and T.E. Wainwright, J.Chem.Phys., 27, 1208, (1957)
[3]. W.G. Hoover and F.H. Ree, J.Chem.Phys., 49, 3609, (1968)
[4]. P.G. Bolhuis, D. Frenkel, S.-C. Mau, and D.A.Huse, Nature., 388, 235, (1997)
[5]. T.C. Hales, P. Sarnak, and M.C. Pugh, Proc. nat. Acad. Sci. USA, 97, 12963, (2000)
[6]. P.N. Pusey and W. van Megen, Nature, 320, 340, (1986)
[7]. W. van Megen and S.M. Underwood, Nature, 362, 616, (1993)
[8]. W. Schaertl and H. Sillescu, J. Stat. Phys, 77, 1007, (1994)
[9]. W. Gotze and L. Sjogren, Phys. Rev. A, 43, 5442, (1991)
[10]. M.D. Rintoul and S. Torquato, Phys. Rev. Lett, **77,** 4198, (1996)
[11]. J. Zhu, M. Li, R. Rogers, W. Meyer, R.H. Ottewill, Crew-Shuttle-Columbia, W.B. Russel, and P.M. Chaikin, Nature, 387, 883, (1997)
[12]. S.I. Henderson, T.C. Mortensen, S.M. Underwood, and W. van Megen, Physica A, 233, 102, (1996)
[13]. G. Bosma, C. Pathmamanoharan, E.H.A. de Hoog, W.K. Kegel, A. van Blaaderen, and H.N.W. Lekkerkerker, J. Colloid Interface Sci., 245, 292, (2002)
[14]. W.K. Kegel, Langmuir, 16, 939, (2000)
[15]. E.H.A. de Hoog, W.K. Kegel, A. van Blaaderen, and H.N.W. Lekkerkerker, Phys. Rev. E, 64, 021407, (2001)
[16]. W.K. Kegel and A. van Blaaderen, Science, 287, 290, (2000)
[17]. A. Yethiraj and A. van Blaaderen, Nature, 421, 513, (2003)
[18]. U. Gasser, E.R. Weeks, A. Schofield, P.N. Pusey, and D.A. Weitz, Science, 292, 258, (2001)
[19]. W. van Megen, T.C. Mortensen, S.R. Williams, and J. Müller, Phys. Rev. E, 58, 6073, (1998)
[20]. N. Simeonova and W.K. Kegel, Faraday Discuss., 123, 27, (2003)
[21]. E.R. Weeks, J.C. Crocker, A.C. Levitt, A. Schofield, and D.A. Weitz, Science, 287, 672, (2000)

5

Devitrification of colloidal glasses in real-space

Abstract

Confocal scanning laser microscopy has been used to quantitatively analyze the structure and dynamics of concentrated suspensions of spherical colloids in which the magnitude of the short range attractive potential is increased by adding non-adsorbing polymers. These systems undergo a reentrant glass transition upon increasing polymer concentration. The melting of the glass is accompanied by significant changes in the displacement distribution and its moments. However, no significant variations have been detected in the shapes of the displacement distributions. Moreover, structural correlation functions and the magnitude of local density fluctuations do not vary significantly between the glass states and the fluid. Considering the experimental setup, these observations imply that local density fluctuations cannot be larger than a few percent of the average density.

5.1 Introduction

Glasses and gels are solids without long-range positional order. A wide variety of molecular and macromolecular systems form glasses (see, e.g., ref. [1], for an overview). A glass state has also been observed in colloidal systems in which only excluded volume interactions play a role, see, e.g., ref. [2, 3]. Colloidal gels often form at relatively low volume fractions of colloids, but only if short range attraction is present (see, e.g., ref. [4]). It has recently become clear, by theory [5], experiments [6, 7, 8] and by computer simulation [9], that glasses of colloidal hard spheres can be 'devitrified' upon increasing attraction between the colloidal particles. 'Devitrification' means that structurally disordered systems that do not reach long-time self diffusion within experimental time scales do so after 'switching on' attraction. Attraction between colloidal particles can be accomplished by adding nonadsorbing polymers, leading to an attractive potential (of mean force) between the colloids [10, 11]. Interestingly, the system again forms a glass state if even more polymer is added [6, 7]. The situation is shown schematically in Figure 5-1. In ref. [7, 8] it has been shown that the peak of the static structure factor shifts to slightly larger q values when the repulsive glass devitrifies. At the same time, the extrapolated value of the static structure factor at q=0 increases. These observations point to local inhomogeneities of the particle density: the shift of the peak of $S(q)$ suggests a decreasing interparticle distance, while the larger values of $S(q = 0)$ suggest an increasing osmotic compressibility. At constant volume, decreasing interparticle distance indeed should locally induce holes of relatively low number densities. Dynamically, this translates into a subset of particles becoming more mobile at the expense of another subset. In this work, this scenario is investigated by analyzing the particle displacement distributions as well as the local particle density distributions using Voronoi constructions.

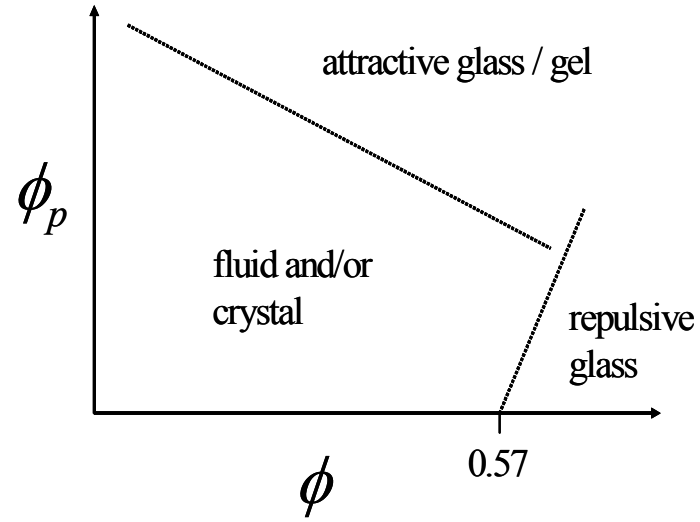

Figure 5-1 Schematic stability diagram of fluid, repulsive glass and attractive glass or gel state as a function of colloid volume fraction Φ and polymer volume fraction Φ_p. Modeled after ref. [6–8]. At constant $\Phi \geq 0.57$ and increasing Φ_p, a sequence repulsive glass - fluid - attractive glass is observed, referred to as a reentrant glass transition.

5.2 Experimental section

Polymethyl methacrylate spheres, consisting of a fluorescent core and a non-fluorescent shell and a relative polydispersity of 6 percent [12, 13] were used. The particles were dispersed in a refractive index matching solvent mixture of cis-decalin, tetralin and carbon tetrachloride with volume fractions of 0.315, 0.36, and 0.325, respectively. The mass density of this solvent mixture is close to that of the particles with a mismatch of $\Delta\rho$ = 0.02g/cm^3 and the interparticle interactions are hard [14, 15]. The diameter d of the particles is 1.45 μm, corresponding to a gravitational length $h = 6kT/(\Delta\rho d^3 g) \approx 13\mu m$ with g the acceleration due to gravity. The volume fraction Φ of the colloids was 0.59 as determined relative to the random close-packed volume fraction as in ref. [14]. Samples contained several concentrations of non-adsorbing polymer, polystyrene (Fluka; molecular weight = 6×10^5 g/mole; radius of gyration $r_g \approx 22$ nm). The volume fractions of the polymer Φ_p ($= 4\pi r_g^3 \rho/3$ with ρ the polymer number density) are equal to 0, 0.010, 0.036, 0.042, 0.063, 0.10, and 0.23. Without polymer, the typical time scale in the system is the Brownian time defined by $\tau_B = r^2/6D_0 = 1.61$ s. Here, r is the radius of a colloidal particle and D_0 is its diffusion coefficient at infinite dilution and no polymer. The last quantity is given by $D_0 = kT/6\pi\eta_0 R$, with η_0 the solvent viscosity. Increasing polymer is expected to

increase the viscosity η of the samples, as a first approximation via the Einstein relation $\eta=\eta_0(1+2.5\Phi_p)$. This implies that the difference in viscosity between the samples with Φ_p=0.23 and Φ_p =0 is roughly 50 percent. Samples were prepared by mixing stock solutions of colloid and polymer. After mixing, the samples have been continuously tumbled for at least three days. Measurements started within one hour after tumbling was finished.

A Nikon TE 2000U inverted microscope equipped with a Nikon C1 confocal scanning head in combination with an HeNe laser (5 mW, 543 nm, Melles Griot) and an oil-immersion lens (100× CFI Plan Apochromat, NA 1.4, Nikon) was used to image the particles. The 2D *xy* cross-section images of approximately 30 particle diameters away from the wall of the sample cell had a resolution of 512×512 pixels and the frame size was 50×50 μm. The optical thickness of a slice, before image analysis, was 0.5 particle diameter. The scan-speed was about one second per frame. The centers of the particles were located using particle tracking routines based on those described in [16]. With this procedure, under optimal conditions a resolution of particle positions of approximately 1/10 of a pixel can be accomplished. Time series were taken over 150 intervals of 30 seconds.

From the retrieved particle positions several properties were determined. First of all, the self part of the van Hove correlation function G_s, was calculated, being the canonically averaged probability distribution that a particle has traveled a distance x in a time interval t

$$\mathrm{G_s(x,t)}=\frac{1}{\mathrm{N}}\left\langle\sum_{i=1}^{N}\delta\left[x+x_i(0)-x_i(t)\right]\right\rangle \tag{5.1}$$

Subsequently, the mobility of the particles was measured in terms of the mean squared displacement $\langle x^2\rangle$, which is defined as the second moment of G_s

$$\left\langle x^2(t)\right\rangle=\sum_{i=1}^{N}x^2(t)G_s(x,t) \tag{5.2}$$

Here and below, all distances are given in units of the particle diameter, unless stated otherwise. The lowest order deviation from a Gaussian displacement distribution for displacements along a single coordinate is given by [17]

$$\alpha^2(t) = \frac{\left\langle x^4(t) \right\rangle}{3\left\langle x^2(t) \right\rangle^2} - 1 \tag{5.3}$$

From the particle positions the radial distribution function and the Voronoi 'volumes' are calculated. The radial distribution function *g(r)* (being proportional to the probability of observing a particle at distance *r* away from a given particle) is given by

$$g(r) = \frac{1}{\rho^2}\left\langle \sum_i \sum_{j \neq i} \delta(\vec{r_i})\delta(\vec{r_j} - \vec{r}) \right\rangle \tag{5.4}$$

with ρ the average number density. The indices *i* and *j* run over all particles. The nearest neighbors of every particle were identified by correlating the particle positions within single frames using a Delaunay triangulation. Using the corresponding Voronoi polygon construction (a Voronoi cell for each particle is defined as the region of points in space that are closer to that particle than to any other particle), the local area (note that 2D slices were analyzed) occupied by a single particle, A_v, was determined (see Figure 5-2). The normalized local area is defined as

$$a_v = \frac{A_v}{\pi R^2} \tag{5.5}$$

and compute the distribution of a_v, p(a_v); the results are presented in the next section.

5.3 Results and discussions

In Figure 5-3 the displacement distributions, eq. (5.1) at three different times and for three different polymer concentrations are shown. The distributions clearly are dynamically heterogeneous, being manifested in non-Gaussian displacement distributions as has also been observed in [14, 18] for concentrated suspensions of hard colloidal spheres. Figure 5-3 demonstrates

that increasing the volume fraction of polymer from Φ_p=0.013 to 0.063 devitrifies the colloidal hard-sphere glass. With increasing the polymer

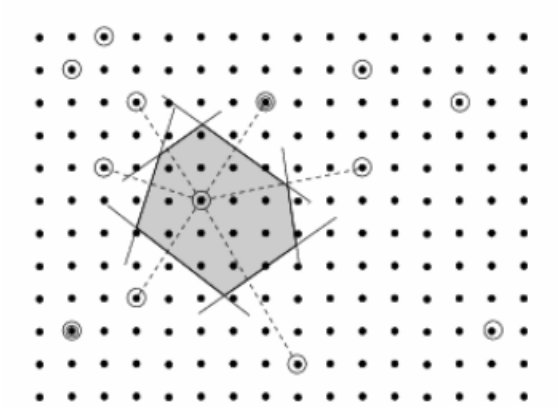

Figure 5-2 Voronoi cell for a particle, defined as the region of space closer to that particle than it is to any other particle. Neighbouring particles are marked with circles.

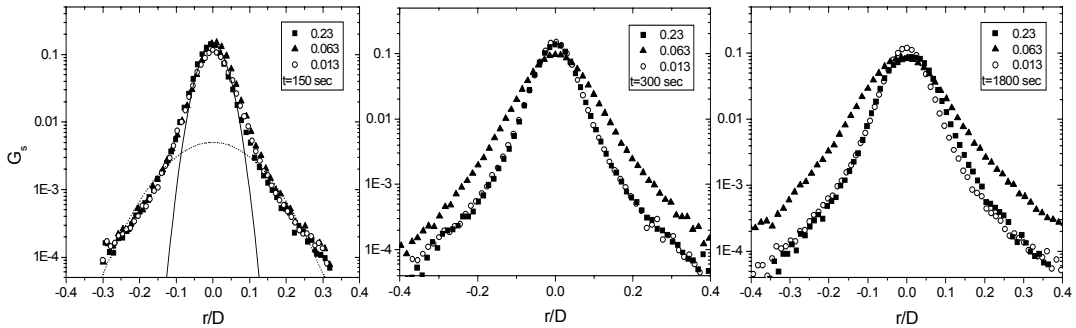

Figure 5-3 Displacement distributions eq. (5-1), at three different times, for samples with colloid volume fraction of 0.59, and three different polymer concentrations: 0.013, 0.063, and 0.23 as indicated in the Figure. Solid lines are Gaussian fits to the (arbitrary) slow and fast subsets of the particles.

concentration even further, i.e., to 0.23, the system again becomes more or less immobile.

As can be seen in the Figure, at t=150s the displacement distributions of all three polymer concentrations are still indistinguishable. At longer times, however, at least beyond 300 s, the displacement distribution of the system with Φ_p=0.063 is substantially broader than samples with both higher and lower polymer concentrations. Thus, the mobility in the sample with intermediate polymer is significantly higher than in the other samples. This

can be verified in Figure 5-4, where the mean squared displacements, eq. (5.2), as a function of time are plotted. Both Figures show that an additional increase of the polymer concentration slows down the system again. The uncertainty in the data in Figure 5-4 is large, caused by the MSD being a second moment of the displacement distribution. By these observations the 'reentrant glass transition as a function of polymer concentration, as also observed experimentally in ref. [6, 7] is verified. At small polymer concentration, the system is a repulsive glass. Upon increasing polymer concentration the system devitrifies, followed by a second ('reentrant') glass transition upon further increase of the polymer concentration.

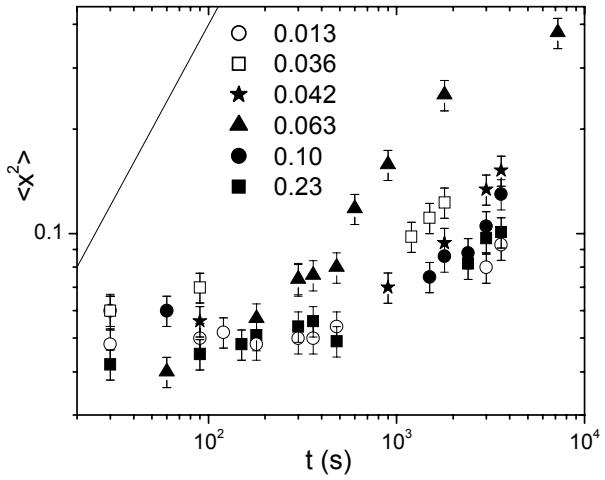

Figure 5-4 Mean-squared displacements calculated by eq. (5.2) for systems with constant volume fraction of colloid (0.59) and increasing polymer concentration. The solid line has unit slope and represents the long-time diffusion limit.

The question if devitrification is accompanied by increased deviations from Gaussian displacement distributions compared to the dynamically arrested systems is addressed. Such deviation is quantified by the value of the non-Gaussian parameter α_2, in eq. (5.3). If devitrification was caused by a subset of particles becoming more mobile at the expense of another subset, a scenario that has been discussed in the Introduction, then a significantly larger value of α_2 would be expected in the system with Φ_p=0.063. This obviously is not the case; in all systems, the value of α_2 as a function of mean-squared displacement fall on the same curve with a (shallow)

maximum around $< x^2 > \approx 0.01$. This behavior is corroborated by inspection of the particle trajectories (see Figure 5-5).

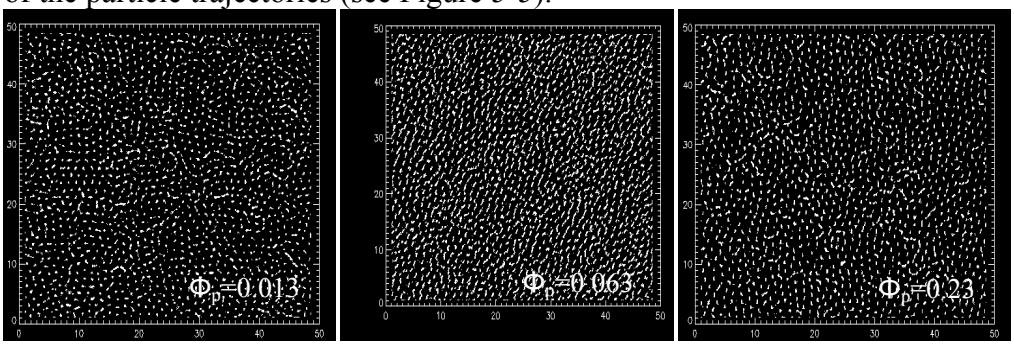

Figure 5-5 Particle trajectories for sistems with different volume fractions of polymer: 0.013, 0.063 and 0.23. From left to right we can observe a repulsive glass, devitrified state, and reentrant glass.

In Figure 5-7 is shown typical configurations of the repulsive glass, the devitrified sample and the attractive glass. From qualitative inspection of these snapshots, one would not be able to tell which sample corresponds to what dynamic situation in the Figures 5-3 and 5-4. In the devitrified samples, crystalline regions were observed several weeks after preparation, but no systematic crystallization study (as in ref. [6, 8]) has been carried out. The structure and the local volume distributions of the systems will be analyzed below.

The pair correlation functions *g(r)*, see eq. (5.4), are shown in Figure 5-8 and the Voronoi distributions are given in Figure 5-9. Clearly, these quantities do not point to significant differences in the real-space structure in these systems. At least in more dilute systems, the first peak of *g(r)* is expected to sharpen with increasing polymer concentration [19], which is not observed in the dense systems studied here. Neglecting excluded volume effects of the polymers, the depths of the attraction wells as a function of polymer concentration are given by $-\beta u = 1/2\ \Phi_p(3/\xi+2)$ with $\xi = 2r_g/d$; see, e.g., [20]. It is easy to verify that $\Phi_p \approx 0.013$, 0.036, 0.042, 0.063, 0.1 and 0.23 corresponds to $-\beta u \approx 0.7$, 1.8, 2.1, 3.2, 5.0, and 11.5, respectively. Comparing these numbers with the results in Figures 5-3 and 5-4, reveals that devitrification occurs when the depth of the attraction well $-\beta u \approx$ 2-3, while the attractive glass forms when $-\beta u \approx$ 3-5. From the data in ref. [8] it can be deduced that at a colloid volume fraction of 0.6, $-\beta u \approx 0.7$ and $-\beta u \approx 1.6$ for the devitrification and reentrant glass transition, respectively. These numbers are significantly smaller compared to those extracted from our data. This may be caused by different ranges of attraction induced by the polymers of

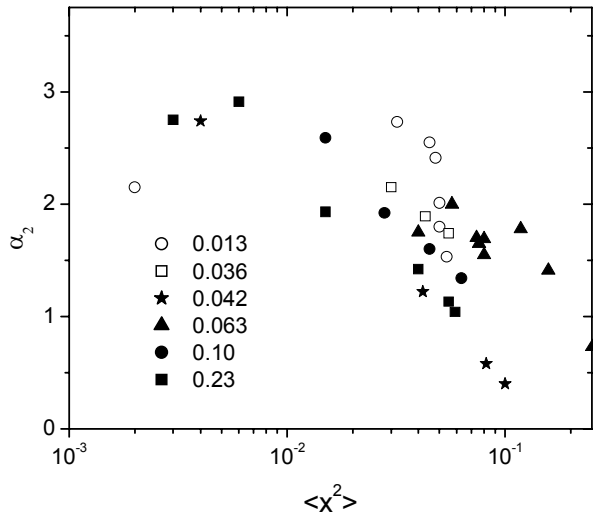

Figure 5-6 Values of the non-Gaussian parameter α_2, given by eq. (5-3) as a function of the mean squared displacement; symbols as in Fig. (5-4)

different radius of gyration in the two experimental setups. Indeed, in ref. [8], $\xi = 0.09$ while in present experiments, $\xi = 0.03$. This points to the fact that the sequence repulsive glass – devitrified state - reentrant glass is shifted to lower polymer concentrations upon increasing the range of interactions. This scenario seems globally in agreement with theory; see ref. [5].

As mentioned in the introduction, in ref. [8] it has been observed that increasing the polymer concentration in the system is accompanied by a shift in the structure factor peak to higher q as well as an increased osmotic compressibility. Upon increasing polymer concentration, these observations may translate into local clustering of particles which, at constant volume, opens up 'holes' on the spatial scale of a few particle diameters. In real-space, this scenario should be reflected in: (1) smaller spacing in the peaks of $g(r)$; (2) broadening in the distribution of Voronoi volumes, or a bimodal distribution of Voronoi volumes. In the last situation, local clustering leads to smaller Voronoi volumes, and the 'holes' lead to larger volumes. It can be verified that the shift of the structure factor peak as observed in ref. [8] corresponds to roughly 5 percent of the particle diameter. Such a small difference will indeed not show up in our measured $g(r)$. Whether it shows up in the distribution of Voronoi volumes depends on the spatial scale of the inhomogeneities. This scale is hidden in the osmotic compressibility, but cannot be extracted from the data in ref. [8]. The results in Figure 5-9 show that inhomogeneities in interparticle spacing (if any), are below the

experimental resolution of the Voronoi volumes. The standard deviation of the positions of the particles under slightly different values of the parameters used in the tracking procedure was measured. These values were chosen in such a way that visually, all particle positions were recovered. With this procedure, it is verified that the resolution of the particle positions in the presented datasets is 1/4 to 1/3 of the size of a pixel (with a size of 50/512 μm), or 25 - 35 nm, two percent of the particle diameter. Voronoi volumes are based on interparticle distances which are in fact projected distances in a vertical slice of finite thickness. The uncertainty in the interparticle distance extracted from these slices may be significantly larger. The thickness of an optical slice is 'normalized' by using refractive index-matched solvent, the same microscopy settings in all experiments, and averaging over several experimental samples. The optical thickness is reduced by discriminating all particles with intensity below 50 percent of the average intensity. With these precautions, the effect of finite slice thickness contributes as a systematic error showing up, e.g., in finite contributions to $g(r < d)$ in Figure 5-8 and in finite $p(a_v < 1)$. Distributions of (averaged) interparticle distances are therefore expected to significantly detect shifts larger than roughly 30 nm.

The data were also analyzed in terms of 'bond' distance distributions. In fact, the $g(r)$'s in Figure 5-8 are radial averages over these distributions. A radial average is not very sensitive for 'clustering' in the form of pairs or linear aggregates of the colloids. However, by comparing the distributions of interparticle distances (not shown), no significant differences showed up. This implies that shifts in local bond distributions are below the experimental resolution of the particle positions, again estimated as 30 nm. How does that compare to the shift of the structure factor corresponding to about 5 percent of the particle size as observed in ref. [7,8]? For the particle size used here, this difference, in this case about 60-70 nm, should show up in the Voronoi distribution, (see Figure 5-7) as well as in the distribution of interparticle distance. The interparticle distance scales as $l = d(\Phi_{rcp}/\Phi)^{1/3}$ with Φ_{rcp} the random close packed volume fraction of 0.64. From that, it is easy to see that differences in volume fraction on the order of 0.01 give rise to differences in interparticle distance of order one percent. Thus, a small uncertainty in volume fraction may partly account for the significant shift of the structure factor peak in ref. [7, 8]. On the other hand, two independent experiments [7, 8] show the same trend, thereby adding weight to the significance of the shift of the structure factor. The systematic increase of osmotic compressibility with polymer concentration, as observed in ref. [7, 8], points to increased

density fluctuations in the system. These fluctuations have not been detected by the present experimental setup, implying that the relative fluctuations in density are smaller than 2-3 percent of the interparticle distances.

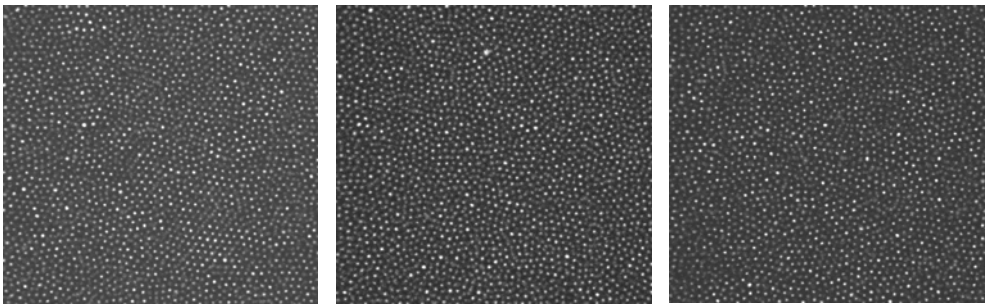

0.013 0.063 0.23

Figure 5-7 Snapshots of systems with different volume fractions of polymer, as indicated. From left to right we have a repulsive glass, devitrified state, and reentrant glass.

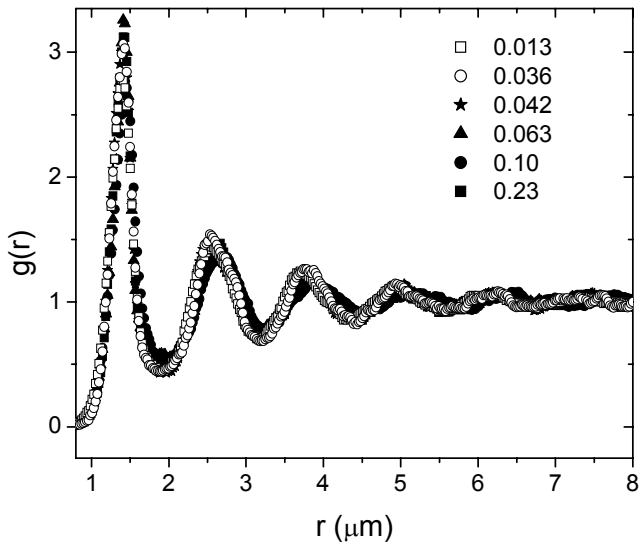

Figure 5-8 Radial distribution functions of the same systems as in previous Figures.

In ending this section, it has to be noted that in ref. [21] a significant influence of gravity on the dynamics of concentrated colloidal hard-sphere dispersions has been reported. There it has been shown that gravity significantly influences aging dynamics if the gravitational length to particle

diameter ratio becomes of order 10 or smaller. In the system studied here, the gravitational length to particle diameter ratio is approximately 9, while in ref. [8] it is roughly 100. The one in the system of swollen micro-sponges studied in ref. [7] probably is even larger than that. Yet, there is no reason to believe that gravity is qualitatively important here. Indeed, in ref. [21] it has been shown that gravity effects become important after much longer waiting times than the ones in this study. Moreover, the results on particle displacements reported here (see Figures 5-3 and 5-4), clearly indicate that .gravity does not qualitatively influence the devitrification scenario as reported by the light scattering studies. Therefore there is no reason to believe that gravity qualitatively influences the coupling to static structure upon devitrification either.

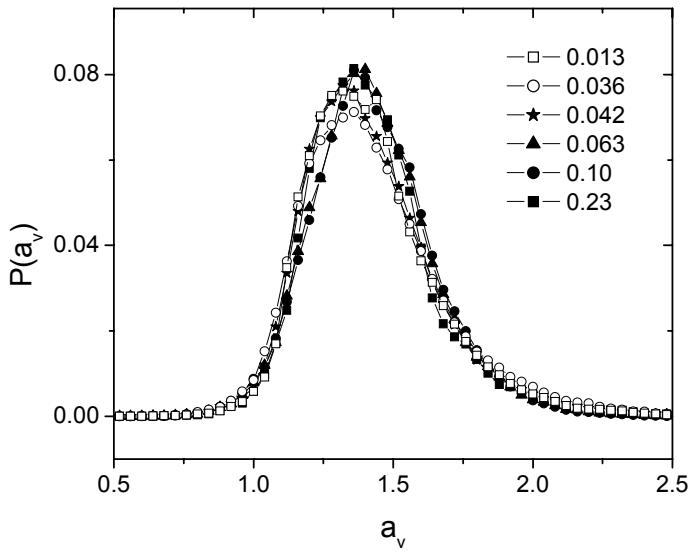

Figure 5-9 Distribution of Voronoi volumes in the same systems as in previous Figures.

5.4 Conclusions

The sequence of repulsive glass - devitrified state – attractive glass was observed in concentrated suspensions of colloidal spheres as a function of increasing interparticle attraction, in agreement with refs. [6, 7]. It was shown that devitrification in real-space is significantly reflected in broadening of the displacement distribution and its moments. Displacement

distributions are non Gaussian. The shapes of the displacement distributions are not significantly different for the two different glass states and the devitrified state. The last observation is reflected in the value of the non-Gaussian parameter α_2. Analysis of structure and local density fluctuations revealed no significant differences between the three situations. Considering the experimental setup, this implies that relative density fluctuations are at most a few percent of the average interparticle distance. Obviously, dynamically, a clear signature of devitrification and revitrification occurs, but significant differences in local structure and density distributions in real-space were not found.

References

[1]. C. A. Angell, Science, 267, 1924, (1995).
[2]. P. N. Pusey andW. vanMegen, Nature, 320, 340, (1986).
[3]. W. Gotze, in Liquids, Freezing, and the Glass transition,edited by J. P. Hansen, D. Levesque, and J. Zinn-Justin, North Holland, Amsterd am, (1991).
[4]. J. Bergenholtz, W. C. K. Poon, and M. Fuchs, langmuir, 19, 4493, (2003).
[5]. K. Dawson, G. Foffi, M. Fuchs, W. Gotze, F. Sciortino, M. Sperl, P. Tartaglia, T. Voigtmann, and E. Zaccarelli,, Phys. Rev. E, 63, 011401, (2000).
[6]. K. N. Pham, A. M. Puertas, J. Bergenholtz, S. U. Egelhaaf, A. Moussad, P. N. Pusey, A. B. Schofield, M. E. Cates, M. Fuchs, and W. C. K. Poon, Science 296, 104, (2002).
[7]. T. Eckert and E. Bartsch, Phys. Rev. Lett. 89, 125701, (2002).
[8]. K. N. Pham, S. U. Egelhaaf, P. N. Pusey, and W. C. K. Poon, Phys. Rev. E, 69, 011503, (2004).
[9]. A. Puertas, M. Fuchs, and M. E. Cates, Phys. Rev. Lett. 88, 098301, (2002).
[10]. S. Asakura and F. Oosawa, J. Chem Phys., 22, 1255, (1954).
[11]. A. Vrij, Pure Appl. Chem., 48, 471, (1976).
[12]. R. P. A. Dullens, E. M. Claesson, D. Derks, A. van Blaaderen, and W. K. Kegel, Langmuir, 19, 5963, (2003).
[13]. R. P. A. Dullens, E. M. Claesson, andW. K. Kegel, Langmuir, 20, 658, (2004).
[14]. W. K. Kegel and A. van Blaaderen, Science, 287, 290, (2000).
[15]. E. H. A. de Hoog, W. K. Kegel, A. van Blaaderen, and N. W. Lekkerkerker, Phys. Rev. E, 64, 021407, (2001).
[16]. J. C. Crocker and D. G. Grier, J. Colloid Interface Sci., 179, 298, (1996).
[17]. B. R. A. Nijboer and A. Rahman, Physica, 32, 415, (1966).
[18]. E. R. Weeks, J. C. Crocker, A. C. Levitt, A. Schofield and D. A. Weitz, Science, 287, 672, (2000).
[19]. J. P. Hansen and I. R. McDonald, Theory of Simple Liquids, Academic Press, London, 2nd ed,(1986).
[20]. H. N. W. Lekkerkerker, W. C. K. Poon., P. N. Pusey, A. Stroobants, and P. B. Warren, Europhys. Lett., 20, 559, (1992).
[21]. N. B. Simeonova and W. K. Kegel, Phys. Rev. Lett., 93, 035701, (2004).

6

Real-space determination of particle displacements parallel and perpendicular to a gravity field in glasses of colloidal hard spheres

Abstract

The influence of gravity on long-time diffusion in glasses of hard colloidal spheres was studied using a new experimental setup that allowed a real space determination of particle displacements in directions parallel and perpendicular to the gravity field. Dispersions of particles were prepared in different solvent combinations that provide different gravitational lengths. It was shown that the direction of the external gravitational field couples to the particle dynamics and influences the values of mean square particle displacements.

6.1 Introduction

Recent computer simulations [1] and experiments under microgravity (in space) [2] pose serious doubts over the existence of a glass transition at volume fractions Φ <0.64 of monodisperse hard spheres in the absence of a gravity field. These studies show that hard spheres crystallize in the absence of gravity up to volume fractions close to 0.64. In [2], a system that is a glass on earth rapidly crystallizes in space after homogenization by mixing. A quantitative study of gravity influence on particle dynamics and aging processes in glassy systems is reported in Chapter 4 [3].

In the present chapter, the interest is focused on the influence of the gravitational field on particles diffusion dynamics in a system of spheres characterized by hard spheres potential, deep in the bulk of the sample. Fluorescent recovery after photo bleaching (FRAP) as an analytical method is applied to analyze particles movements in planes parallel or perpendicular to the direction of the gravity force. The competition between gravity force and particles Brownian motion (entropy), results in different values for mean square particle displacements (MSD) in these two (perpendicular to each other) analytical planes. Confocal scanning laser microscopy (CSLM) as a method for real space and time observations is used. In contrast to the experiments described in Chapters 4 and 3 [3,4], here a new experimental setup is presented, that allows to bleach a cube, and to analyze the development of the intensity profiles in the directions parallel and perpendicular to the external field simultaneously. In all the experiments, bleached cubes were situated far from the cell bottom, at least 30 particle diameters. The above condition was chosen in order to avoid the influence, on particle dynamics, of particles concentration gradient, that can appear as a result of sedimentation [5].

6.2 Experimental

Two sizes of NBD (4-methylaminoethylmethacrylate-7-nitrobenzo-2-oxa-1,3-diazol), labeled Polymethylmethacrylate (PMMA) particles, stabilized with poly(12-hydroxystearic acid) were used in the experiments – 265nm and 295nm in radius. The polydispersity of the particles is about 7%, which prevents spontaneous crystallization, at least in the reported experimental time scales. As described previously in Chapter 4 [3], the

particles were dispersed in two different solvent mixtures providing two different gravitational lengths. The density-matched mixture of cis-decalin, tetralin and carbon tetrachloride with volume ratios 31.5: 36.0: 32.5 respectively, provide a density difference between particles and the solvent of 0.02 g/ml and respectively a gravitational length of 0.1mm. The system of particles dispersed in such a mixture is addressed here as to be under "low gravity" conditions. The solvent combination which provides density difference between the particles and the solvent of 0.3 g/ml and much smaller gravitational length -13μm, is a mixture of cis-decalin and tetralin with volume ratios 68.0: 32.0. Here, is referred as to "normal gravity" conditions. As shown in refs. [6, 7, 8], in these solvent mixtures particles behave as hard spheres and are refractive index matched. There are no indications for the presence of charge [6, 7]. The colloidal mixture of particles and solvent was placed in a specially designed experimental cell. The cell is constructed of a 4 ml capped cylindrical glass vial, which is partially cut off, and at the place of the missing vial wall, a microscope cover glass with a thickness of 0.17 mm was glued (see Figure 6-1(B)).Via centrifugation, the colloidal system was quenched to the random close packing for hard spheres (volume fraction Φ =0.64) and later on diluted to the required volume fractions. The experiments were done with the following volume fractions of particles: 0.45, 0.48, 0.59 and 0.61. It was found that at low volume fractions, where the system is in a fluid phase (Φ = 0.45 and 0.48), due to the relatively short experimental time scales (10^3-10^4 in Brownian time units) and fast particle dynamics, the gravity does not couple to the mean square particle displacements (MSD), whereas at glassy volume fractions (Φ = 0.59 and 0.61), particles long-time diffusion is found to be gravity dependent.

A Confocal Scanning Laser Microscope (CSLM) was employed for bleaching and scanning profiles with a cubic shape and dimensions of 10 to 100 particle diameters in the focal plane, and order of 10 diameters in thickness. The setup differs from the one described in Chapter 3 [4] with its horizontal positioning Figure 6-1(A). The microscope objective was situated horizontally towards the wall of the experimental cell. Such a construction allows performing a microscope scans in the plane parallel to the gravity field as well as perpendicular to it. The cubes were bleached in the sample by applying a maximum laser intensity of 2 mW at λ=488nm perpendicularly to the gravity field direction and later on were imaged at 15% of the maximum laser intensity by scanning several slides, again perpendicular to the field of gravity at different times. The fluorescent intensities were integrated along all

four sides of the bleached cubes and the intensity profiles were obtained. The decay length of the fluorescent intensity profile, defined by the length where the intensity is half the (normalized) intensity of

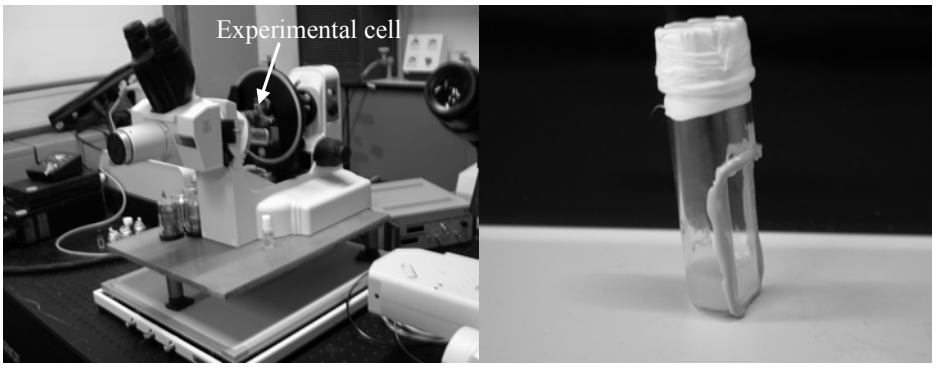

A B

Figure 6-1 Experimental setup A and experimental cell B

the unbleached part of the sample, $x_{1/2}$, is related to the mean squared displacement, $<x^2>$, by :

$$< x^2 > \approx 2.20 x_{1/2}^2. \tag{6.1}$$

In the analysis, the data are fitted to

$$I(x) = \frac{1}{2}(1 - erf\left(\frac{x}{2\sqrt{b}}\right)), \tag{6.2}$$

where b is related to the half width of the laser beam (if the half width is σ then $b = \sigma\sqrt{2}$). The detailed method of analysis is described in Chapter3[4].

In contrast with results obtained in Chapter 4 [3], in this work particle movements are followed in two perpendicular to each other directions. Part of the movements is detected in direction perpendicular to the gravity field (see Figure 6-2) (referred to as ⊥(perpendicular)). The directions of particles movements are shown in the figure with double arrows. The data with regard to the mean squared particle displacements (MSD) obtained for these particles should reproduce the data reported in Chapter 4 [3] since in that case, as well, only perpendicular to the gravity movements could be detected. Other component of the particle movements (referred to as|| (parallel)) is analyzed in plane parallel to the gravity field (dotted double arrow in the

figure). This gives us the opportunity to follow particles dynamics influenced by both, Brownian motion and gravity.

As a result of the presence of gravity, a concentration gradient of particle density could appear at the bottom of the experimental cell [5].To avoid the influence of its presence on the results obtained for $<x^2>$, all the experiments are done far from the cell bottom (30 particle diameters).

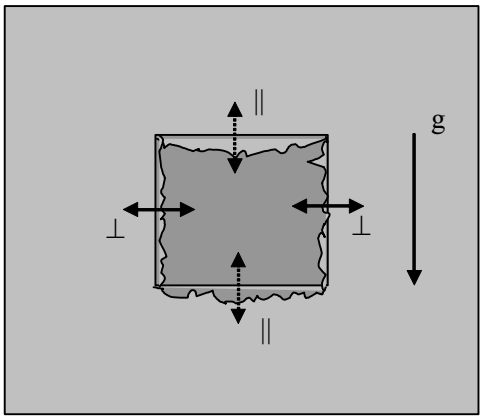

Figure 6-2 Sketch of a bleached cube. The light gray color represents the fluorescent particles, the dark gray is the bleached region. Here ⊥ sides of the cube are sides where particles movements (double arrows) are analyzed in direction perpendicular to the direction of the field and || sides – where the direction of the movements (dotted double arrows) is detected in direction parallel to the field.

6.3 Results and discussions

The mean square particle displacements (MSD) are presented in units of squared particle radius, and time in units of Brownian time where - $\tau_B=r^2/6D_0 \approx 0.059$s, for particles with a radius r= 295nm and τ_B=0.043s for particles with a radius r=265nm. Here, D_0 is the diffusion coefficient at infinite dilution.

In order to illustrate the effect of gravity on a bleached cube, in Figure 6-3, examples of bleached cubes in a sample with a volume fraction of 0.45 over different time intervals are given. Figures 6-3(A-C) represent a sample of particles in density matched solvent, i.e., at low gravity. The times are as follows: (A) is an image taken after $1.7*10^2$, (B) – after $8.4*10^3$ and (C) – after $1.7*10^4$ Brownian times. Figures 6-3(D-F) correspond to a sample at normal gravity (in density non matched solvent) with the following time

scales: (D) - $1.7*10^2$, (E)- $8.4*10^3$ and (F)- $1.7*10^4$ Brownian times. For such samples the time scale for making series of scans is very limited due to the fast particles dynamics. The bleached cube looses its shape and the applied method for image analysis (integration over the intensity profiles) becomes inaccurate, which explains also the scattering in the values of MSD (see Figure 6-6). In the case of a bleached cube at normal gravity, see Figure 6-3(D-F), it looks like the cube "sinks". The reason for such "sinking" could be the presence of gravity field or purely mechanical - movement of microscope stage. If it is a gravity effect taking place on such short time scales ($1.4*10^7$ Brownian time), a concentration gradient would appear in the sample, which would influence the analyses. It would find an expression as an asymmetry in the development of the parallel to the gravity intensity profiles. So far no such behavior was detected during the analyzes. The effect of the "sinking" does not interfere with the further image analyzes since the fluorescent intensities were integrated along both parallel to gravity sides of the bleached cube and the (normalized) intensity profiles were obtained. For the samples with volume fractions of particles at glass transition concentration, no changes in the cube profile can be detected directly from the microscope image due to its small displacement and the big time scale at which this displacement occurs. Therefore, images for this case are not presented here.

To illustrate better the applied method for analysis, in Figure 6-4 the intensity profiles and their error function fits derived form the images in Figure 6-3 along the $\perp$ and || sides of the bleached cubes, are presented. As it can be seen from Figure 6-4, the intensity profile development is comparable in both cases- low gravity and normal gravity. Moreover, there is no significant difference in the development of the perpendicular and parallel profiles. The MSD results for system with volume fractions of 0.45 and 0.48 are presented below in Figure 6-6 (A) and (B).

For systems at glass transition volume fractions the profile analysis for the parallel to the gravity field side of the cube may be compromised if the intensity front of the bleached cube is deformed under the influence of the shear created by collective particle movements caused by gravity presence. This wouldl lead to incorrect values of the $<x^2>$. That is why it is important to check the development of the shape of the intensity front for the parallel to the gravity sides of the cube. The situation is principally different with respect to perpendicular to the gravity sides of the cube, where the direction of the shear would be perpendicular to the direction of the analyzed particle

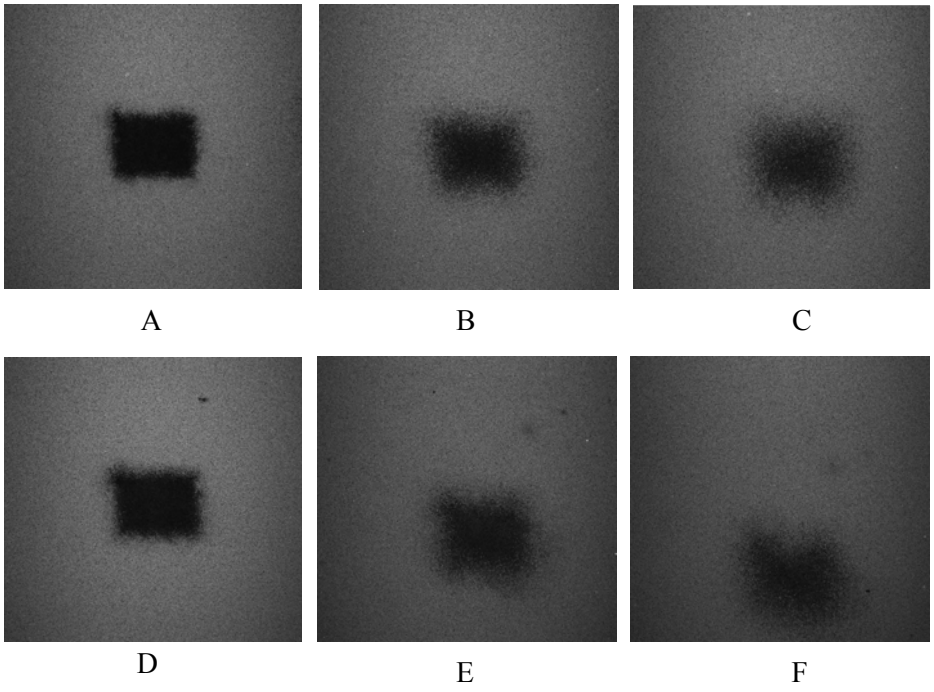

Figure 6-3 Example of bleached cubes at different time intervals in samples with volume fraction of particles of 0.45. A-C at low gravity (density matched solvent), D-F at normal gravity (density non matched solvent). Scanning times are as follows: A is an image taken after $1.7*10^2$; B – after $8.4*10^3$; C – after $1.7*10^4$; D – after $1.7*10^2$; E- after $8.4*10^3$; F- after $1.7*10^4$ in Brownian time units

movements (for the simplest flow fields) and therefore would be undetectable during the profile development.

A single image, for a sample at glassy volume fraction Φ=0.61, was divided in to narrow slices (5 particle diameters each, as it shown in the upper of the Figures 6-5 (B)), situated parallel to gravitational field that could be analyzed as independent images. Integration of the particle intensity was made for each slice of the image at short moment after the bleaching and after $1*10^7$ Brownian time. The displacements for each slice were compared at two times respectively. In Figure 6-5 (A), the displacements of all twelve slices are plotted and represent the profile of the front line of diffusing particles. In Figure 6-5 (B) images of the bleached sample are shown at both scanning times. As seen from Figure 6-5 (A), the parallel bleached profiles do not deform at the timescale of our interest and the results for MSD will not be compromised.

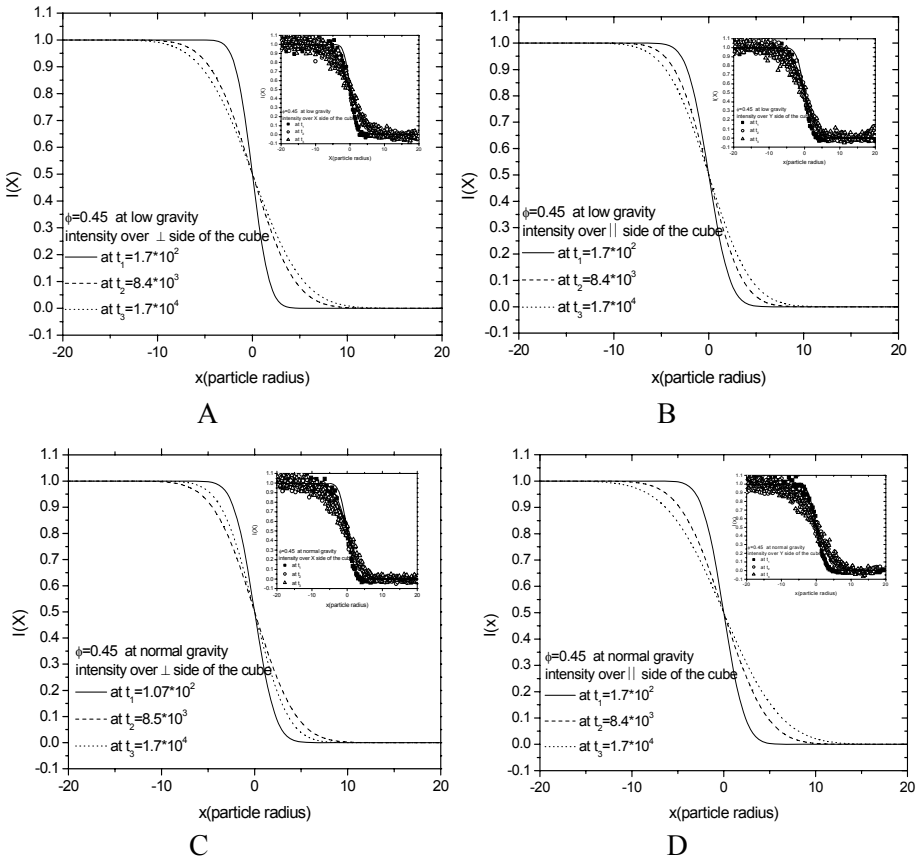

Figure 6-4 Error function fits to the normalized intensity profiles (see the insets) for system with Φ=0.45 under low (A and B) and under normal gravity (C and D), representing the development in time of the intensity front in planes perpendicular and parallel to the gravity field direction.

In Figure 6-6, the results for the mean square particle displacements for the systems with low volume fractions of 0.45 (see Figure6-6(A)) and of 0.48 (see Figure 6-6(B)) of particles under low and normal gravity are presented. The results clearly indicate that at these relatively low volume fractions there are no significant differences between the systems in a density matched and in a density non matched solvent. As it was discussed already in Chapter 4 [3], these systems are at the long-time diffusion limit and the values for particles MSDs for the parallel and the perpendicular to the gravity sides of the cube, are characterized by unit slope – plotted with a dotted line in the Figure 6-6. This is a clear indication that particles diffusion is not influenced by the gravity presence, at least at the experimental time scales of interest.

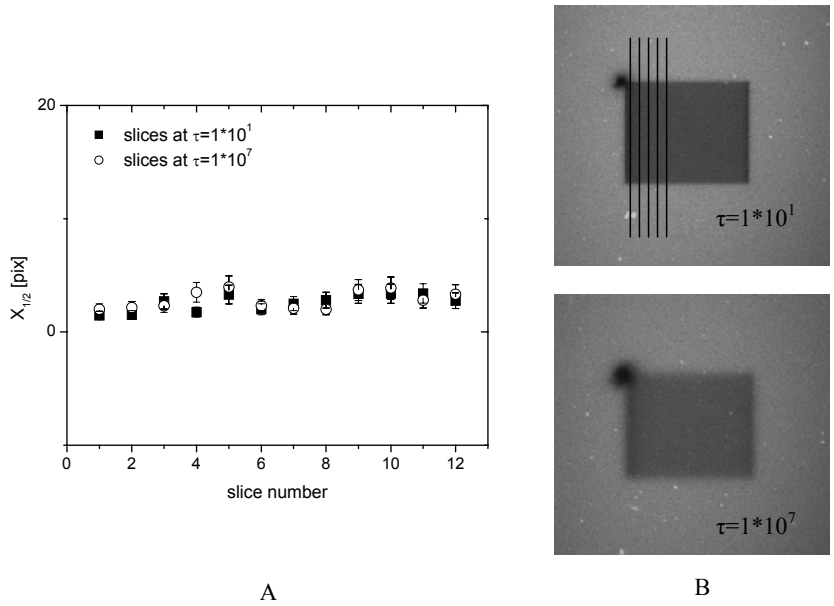

A B

Figure 6-5 Example of || profile development (A) at Brownian times corresponding to $1*10^1$ - closed squares and $1*10^7$ – open circles. (B) - the images corresponding to the same Brownian times in a glassy system.

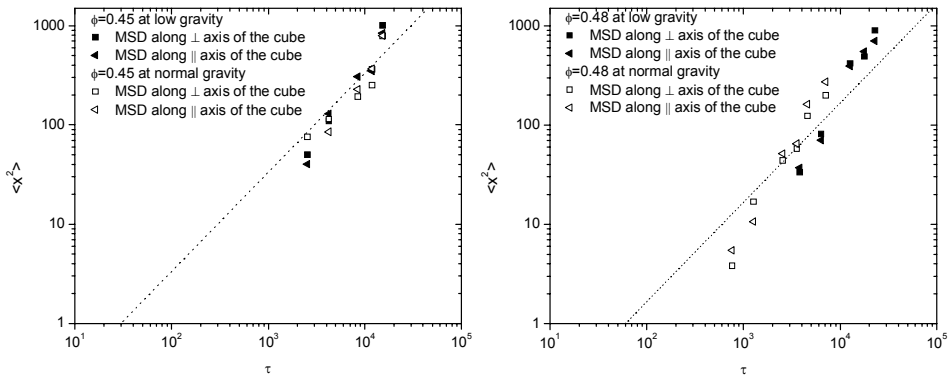

A B

Figure 6-6 Mean square displacements for systems with volume fractions of particle 0.45 -A and 0.48 -B in units of the squared particle radius versus time in units of Brownian time units. The closed squares represents the data for ⊥ sides of the analyzed cubes at low gravity, the closed triangles are the data for || sides at low gravity. The open symbols represent, respectively, the data at normal gravity – squares – for the ⊥ sides, triangles – || sides. The dotted line is with a unit slope, characteristic for long time diffusion limit.

The data for the systems at low gravity are consistent with those reported earlier in Chapters 4 and 3 [3], [4], where particles motion is detected only in direction perpendicular to the direction of the external field due to the experimental setup conditions.

The situation is principally different in cases of samples around the glass-transition volume fractions where gravity effects particles mobility and dramatically accelerates systems aging [3]. This effect is expected to lead to difference in the integrated intensity profiles perpendicular and parallel to the external field and respectively in the values for MSD. The profiles at t_1 (obtained at the moment right after the bleaching) for $\Phi = 0.59$ and $\Phi = 0.61$ are shown in Figures 6-7(A) and 6-7(C), respectively. The same profiles, but at moment t_2 (approximately $3*10^5$ after t_1) are presented in Figures 6-7(B) and 6-7(D), respectively. In the figure, the difference in the development of $\perp$ and || profiles is not well pronounced, or at least it is difficult to detect it just from the profiles images. However, the error function fits to these profiles, reveal a difference (between $\perp$ and || profiles) of 0.04 particle radii (10.6 nm) at t_1 and 0.21 particle radii (55.65 nm) at t_2 for $\Phi = 0.59$. For volume fraction of 0.61, the difference is 0.125 particle radii (33.13 nm) at t_1 and 0.22 particle radii (58.3 nm) at t_2. These, small at first sight differences, lead to a difference of an order of magnitude between the values of MSD along $\perp$ and || sides of the bleached cube.

In Figures 6-8 and 6-9, the results for MSD for glassy systems at low gravity and normal gravity respectively are shown. The data reported in Chapter 4 [3] are added to the plots in order to compare with the recent findings.

In Figures 6-8(A) and (B), the data for systems at low gravity conditions are presented for $\Phi = 0.59$ and $\Phi = 0.61$. For each bleached cube, all four intensity profiles are integrated (two perpendicular and two parallel). The averaged data for $\perp$ sides and || sides are presented. The MSD of the particles along perpendicular and parallel sides of the cube for $\Phi = 0.59$ (see Fig. 6-8(A)) are consistent with the data found earlier and reported in Chapter 4 [3] when the analysis was done in the plane perpendicular to the gravity field. In the reported experimental time scale, particles in such system diffuse about 1-2 particle diameters in space. At times $>10^7$ Brownian time, the effect of aging of the system appears.

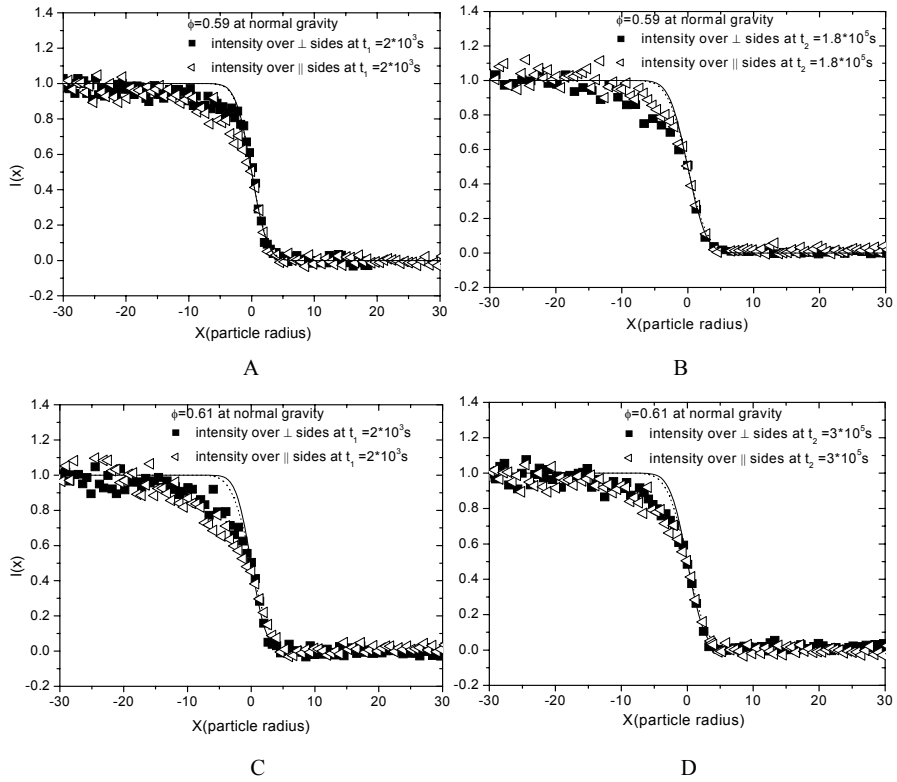

Figure 6-7 Normalized intensity profiles for systems under normal gravity representing the perpendicular to the gravity field sides of the bleached cubes – closed squares and parallel to the field sides of the cubes – open triangles. A and B correspond to Φ=0.59 and C and D to Φ =0.61.The profiles in A are taken at the first scanning moment after the bleaching $t_1=2*10^3$, in B same profiles are taken after a waiting time of $1.8*10^5$. The profiles in C are again taken at first scanning moment $t_1=2*10^3$ and in D the same profiles are taken after a waiting time of $3*10^5$ in Brownian time units.

Very similar is the situation for Φ = 0.61 (see Figure 6-8(B)). The small difference in the data for Φ = 0.59 and Φ = 0.61 is only in the distance that particles can diffuse for comparable time scales. That is due to the difference in the volume fraction concentration (see also Chapter 4 Figure 4-1).

In comparison to the systems at low gravity, for systems at normal gravity, the presence of the gravitational field should influence the particles diffusion according to the results reported in Chapter 4 [3]. In figure 6-9(A), the data for Φ = 0.59 are plotted. It is clear that the mean square particle are plotted. It is clear that the mean square particle displacements along the perpendicular and the parallel sides of the cube are both influenced by the

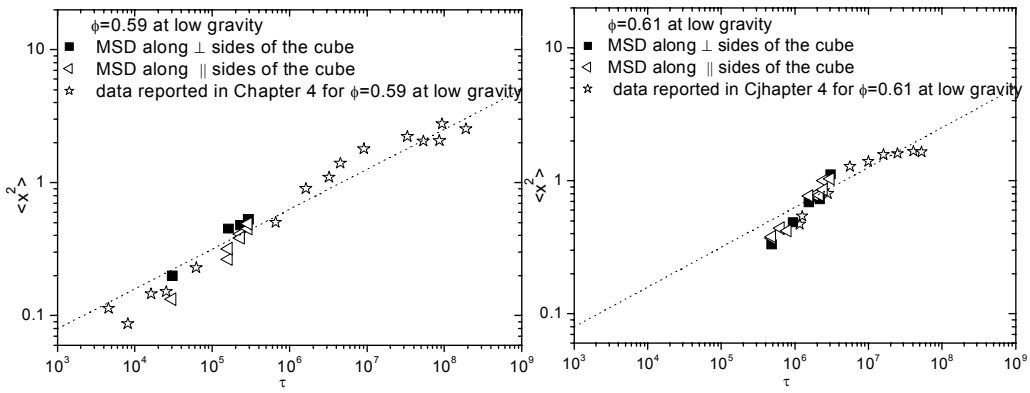

A B

Figure 6-8 Mean square displacements for systems at low gravity with volume fractions of particle 0.59 -A and 0.61 -B in units of squared particle radius versus time in Brownian time units. The closed squares represents the data for ⊥ sides of the analyzed cube, the open triangles are the data for || sides. The open stars correspond to the data obtained earlier and reported in [3]. The dotted line represents a slope of 0.3, discussed in [3]

presence of the external field, compared to the data at low gravity. The data for the diffusion of the particles in the plane perpendicular to the external field are in good agreement with the ones reported in Chapter 4 [3]. This can be expected, because in both cases, the scan is performed perpendicular to the direction of the gravity field, where only the diffusion component of the particle motion is detected.

In the case when particle movements are analyzed in direction parallel to the gravity field, the gravity force and the diffusion, both contribute to the measured values of MSD. At equal times the values for MSD along the perpendicular and parallel sides of the bleached cube differ approximately with an order of magnitude. This result is reproducible for a glassy system with Φ = 0.61 (see Figure 6-9(B)). A possible explanation is that gravity couples to the particle movements involving many particles, with mechanism compared to shear inhomogeneities [9] as its relaxation is much faster in direction parallel to the gravity field. Another possible scenario is the appearance of dynamical heterogeneities [8, 10] which appears on much longer lengthscales in direction parallel to the gravity field compared to the

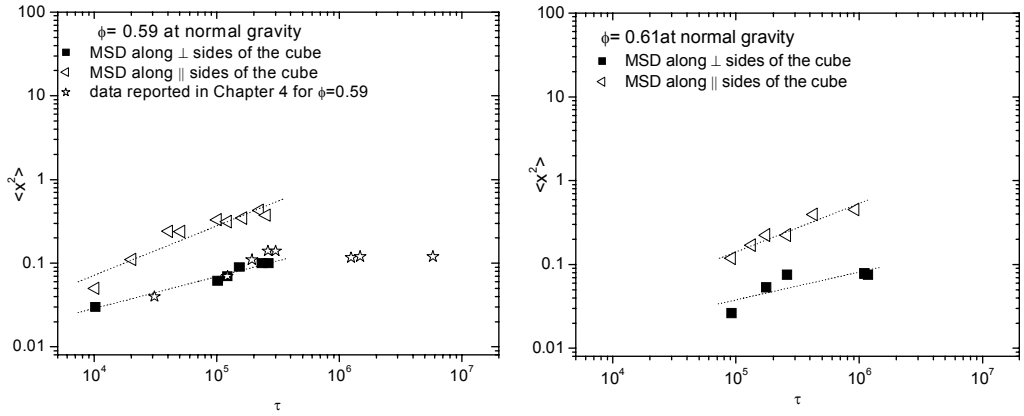

A B

Figure 6-9 Mean square displacements for systems at normal gravity with volume fractions of particle 0.59 - A and 0.61 - B in units of the squared particle radius versus time in units of Brownian time. The closed squares represents the data for ⊥ sides of the analyzed cubes, the open triangles are the data for || sides. The open stars in A correspond to the data reported in [3]

one perpendicular to it. These two possible scenarios can be verified by performing an experiment using a microscope and core-shell particles which provide a resolution on a single particle level [8].

To exclude sedimentation as a possible reason for different values of MSD, the intensity profiles along both || to the gravity field sides of a single bleached cube need to be compared. If the sedimentation is responsible for the deviation in the results, then the development of the profiles with the time should be asymmetric with respect to the $x=0$, due to the appearance of concentration gradient in the samples. The profile for the "bottom", parallel to the gravity, side of the cube should show smaller displacements due to the higher local particle concentration.

During the performed analyses on the images of the bleached cubes, no asymmetries in the development of the parallel sides were detected. An example of profile development for a sample with volume fraction of particles 0.61 is shown in Figure 6-10.

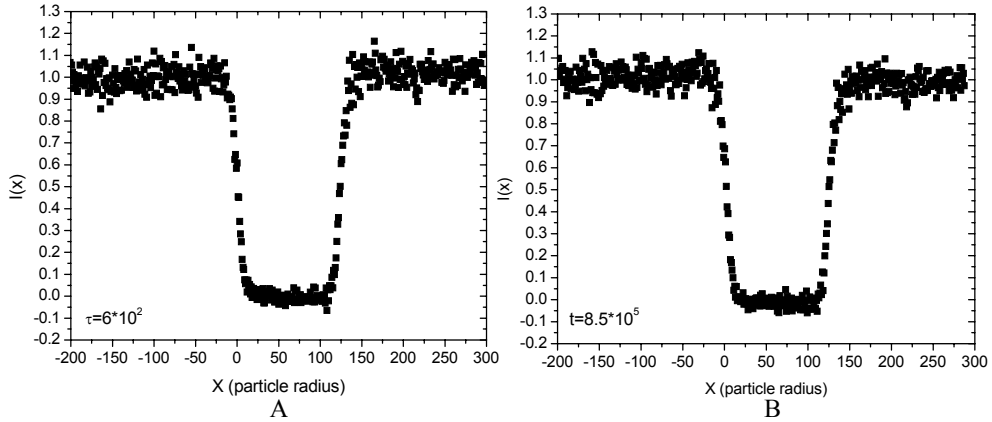

Figure 6-10 Normalized intensity profiles of the parallel to gravity sides of a cube in a sample with Φ=0.61 over different time intervals. A - at $6*10^2$ and B- $8.5*10^5$ in Brownian times.

From the figure it can be seen that the left and the right sides of the profiles, which correspond to the two parallel to the gravity field sides of a bleached cube (see Figure 6-2) are symmetric with respect to the 0-position along the *x*-axes of the plot (the position is chosen according to the analyses procedure described in Chapter 4 [3]).

6.4 Conclusions

The influence of the direction of a gravity field on particle dynamics in glassy colloidal systems was investigated. The method of real-space fluorescent recovery after photo bleaching has been applied to study the particles displacements. The findings confirm the suggestion, referred to in Chapters 4 and 3 [3, 4], that the presence of external field influences the particle dynamics. Particle displacements parallel to the gravity field are "faster" then a displacements perpendicular to it. From the symmetry in the intensity profiles for the parallel sides of a bleached cube after a long period of time, it can be concluded that gravity does not influence particle movements by "simple" sedimentation. It could be that gravity couples to the particle movements involving several particles at the same time. A possible mechanism is shear inhomogeneities [9] as its relaxation is expected to be much faster in the direction parallel to the gravity field due to the gravity

force contribution. Another possible scenario is the appearance of dynamical heterogeneities [8, 10] which appears on much longer lengthscales in direction parallel to the gravity field. These two possible mechanisms can be checked by resolving single particle coordinates [8, 10].

References

[1]. M.D. Rintoul and S. Torquato, Phys. Rev. Lett., 77, 4198, (1996)
[2]. J. Zhu, M. Li, R. Rogers, W. Meyer, R.H. Ottewill, Crew-Shuttle Columbia, W.B. Russel, and P.M. Chaikin, Nature., 387, 883, (1997)
[3]. N. B. Simeonova and W. K. Kegel, Phys. Rev. Lett., 93,035701 (2004)
[4]. N. Simeonova and W.K. Kegel, Faraday Discuss., 123, 27, (2003)
[5]. T.Biben, J-P.Hansen and J-L. Barrat, J.Chem.Phys.,98,7330 (1993)
[6]. P.N. Pusey and W. van Megen, Nature. 320, 340, (1986)
[7]. E.H.A. de Hoog, W.K. Kegel, A. van Blaaderen, and H.N.W.Lekkerkerker, Phys. Rev. E, 64 021407, (2001)
[8]. W.K. Kegel and A. van Blaaderen, Science., 287, 290, (2000)
[9]. W. van Megen and S.M. Underwood, Nature., 362, 616, (1993)
[10]. E.R. Weeks, J.C. Crocker, A.C. Levitt, A. Schofield, and D.A. Weitz, Science, 287 672, (2000)

Summary

When a colloidal hard sphere fluid is rapidly quenched to a volume fraction of particles approximately equal to 0.58, the system exhibits a transition to a so called colloidal glass. This thesis reports results from a study of particle dynamics in colloidal glasses in the absence and presence of a gravitational field. It also investigates the reentrant glass transition. All the experimental results are obtained after a real space analysis using a confocal scanning laser microscopy as experimental technique.

A general introduction is presented in Chapter 1. It contains a short historical overview of colloidal science and a scope of the particular problems addressed in this thesis. Chapter 2 introduces confocal laser scanning microscopy as an advanced experimental method applied for studying colloidal systems.

In Chapter 3 a new real-space technique that significantly widens the time window over which colloidal systems can be studied, was used. A fluorescent recovery of bleached regions in concentrated suspensions of fluorescent colloidal hard spheres was followed in real space. This method provided data for mean squared particle displacements up to time scales that are three orders of magnitude beyond those available by present experimental techniques like dynamic or static light scattering. It was shown that, above the (hard sphere) glass transition density, particles move over distances on the order of their own diameter on time scales of 10^6 to 10^8 Brownian times. Moreover, the mean squared displacement showed power-law behavior over seven time decades. This behavior is different from earlier observations by dynamic light scattering. It was argued that these differences are caused by gravity effects, as the only difference between the studied systems was the buoyant mass of the colloids.

Further on, the influence of gravity on the long-time behavior of the mean squared displacement in glasses of colloidal hard spheres was studied and results are reported in Chapter 4. Again, real-space fluorescent recovery after photo bleaching has been employed. For the first time, a significant influence of gravity on the mean squared displacements of the particles was presented. In particular, the systems which are glasses under gravity (with a gravitational length on the order of tens of micrometers) showed anomalous diffusion over several decades in time if the gravitational length is increased by an order of magnitude. No influence of gravity was observed in systems

below the glass transition density. It was shown that this behavior is caused by gravity dramatically accelerating aging in colloidal hard sphere glasses. This behavior explained the observation that colloidal hard sphere systems which are a glass on earth rapidly crystallize in space.

A quantitative analysis of the structure and dynamics of concentrated suspensions of colloids in which the magnitude of the short range attractive potential was increased by adding non-adsorbing polymers is reported in Chapter 5. These systems undergo a reentrant glass transition upon increasing polymer concentration. The melting of the glass is accompanied by significant changes in the displacement distribution and its moments. However, no significant variations were detected in the shapes of the displacement distributions. Moreover, structural correlation functions and the magnitude of local density fluctuations did not vary significantly between the glass states and the fluid. Considering the experimental setup, these observations implied that local density fluctuations cannot be larger than a few percent of the average particle density.

Finally, in Chapter 6, the influence of gravity on long-time diffusion in glasses was studied using a new experimental setup that allowed a real space determination of particle displacements in directions parallel and perpendicular to the gravity field. Dispersions of particles were prepared in different solvent combinations that provide different gravitational lengths. It was shown that the direction of the external gravitational field couples to the particle dynamics in concentrated colloidal suspensions and influences the values of mean square particle displacements.

Samenvatting

Colloïden zijn een mengsel van twee stoffen - gedisperseerde fase en dispersie (continu) media. Om een systeem als "colloïdaal" te categoriseren, dient de typische grootte van de deeltjes van de gedisperseerde fase tussen de 1 en 1000 nm te zijn. Een interessante eigenschap van colloïden is dat ze in suspensie overgangen laten zien tussen vloeistof, vaste, en glasachtige fasen; vergelijkbaar met atomen en moleculen.

Indien een colloïdale vloeistof snel gecomprimeerd wordt tot een deeltjes volume fractie van ongeveer 0,58 volumeprocent, zal het systeem een overgang vertonen naar een zogenaamde colloïdaal glas. Een dergelijk systeem wordt gekenmerkt door een ongeordende structuur; deeltjes worden willekeurig omsloten door hun buren.

Dit proefschrift behandelt de dynamica van deeltjes in colloïdale media onder invloed van het gravitatieveld. Verder worden ook de resultaten besproken van het onderzoek naar reentrante glasovergang.

Een algemene inleiding wordt beschreven in Hoofdstuk 1. Het bevat een kort historisch overzicht van de colloïdale wetenschap en het geeft een overzicht van specifieke problemen die later behandeled zulen voerden in de proefschrift. In Hoofdstuk 2 wordt Confocale Laser Scanning Microscopie geintroduceerd; een geavanceerde optische experimentele methode die toegepast wordt om colloïdale systemen in real time te bestuderen.

Via een nieuw ontwikkelde real-space techniek (Hoofdstuk 3) kunnen de colloïdale systemen bestuderen wordend in een aanzienlijk verruimd tijdsinterval. Het herstel van fluorescente front van deeltjes, die in een geconcentreerde colloïdale suspensie met een laser belicht waren, werd gevolgd in het reële ruimte- en tijdsdomein. Deze methode verstrekt gegevens over de gemiddeld kwadratisch verplaatsing van de deeltjes tot een tijdsinterval dat drie ordes groter is dan de beschikbare experimentele technieken zoals dynamische of statische lichtverstrooiing. Er is aangetoond dat bij een dichtheid boven de glasovergang, deeltjes afstanden afleggen in de orde van hun eigen diameter op een tijdschaal van 10^6 tot 10^8 Browniaanse tijdseenheden. Bovendien bleek de gemiddeld kwadratisch verplaatsing exponentieel gedrag te vertonen over meer dan zeven decades. Dit gedrag wijkt af van eerdere analyses via dynamische lichtverstrooiing. Als argument werd aangevoerd dat deze verschillen veroorzaakt worden door gravitatie

Verder, werd de invloed van de gravitatie op het lange termijn gedrag van de gemiddeld kwadratisch verplaatsing in colloidale glas onderzocht, waarvan de resultaten gerapporteerd worden in Hoofdstuk 4. Aangetoond is dat er een belangrijke invloed van de gravitatie op de gemiddeld kwadratische verplaatsing van de deeltjes in geconcentreerde colloïdale systemen bestaat. In het bijzonder, de systemen die zich in de glasfase bevinden, bleken abnormale diffusie van deeltjes te vertonen onder lage gravitatie condities. Geen invloed van de gravitatie werd waargenomen in systemen verkerend beneden de glasovergang. Dit gedrag verklaarde de waarneming dat colloïdale systemen die een glas op aarde zijn, snel kristalliseren in de ruimte.

Een kwantitatieve analyse van de structuur en dynamiek van geconcentreerde colloïde suspensies, waarbij de omvang van de korte afstand aantrekkingspotentiaal werd verhoogd door toevoeging van niet-adsorberende polymeren, wordt toegelicht in Hoofdstuk 5. Deze systemen worden onderworpen aan een reëntrante glasovergang doormiddel van het verhogen van de polymeerconcentratie. Het smelten van het glas gaat gepaard met significante veranderingen in de verplaatsing distributie en zijn momenten. Desalniettemin, zijn er geen significante verschillen in de vorm van het verplaatsingsdistributies waargenomen. Structurele correlatie functies en de magnitude van de plaatselijke dichtheid schommelingen vertoonden geen significante variatie tussen het glastoestanden en de vloeistof. Uitgaande van de experimentele opstelling, impliceren deze waarnemingen dat de lokale dichtheidschommelingen niet groter kunnen zijn dan enkele procenten van de gemiddelde deeltjesdichtheid.

Ten slotte, zal in Hoofdstuk 6 de resultaten besproken worden van de studie naar de invloed van de gravitatie op de lange termijn diffusie in glas. Met behulp van een experimentele opstelling zijn de real space deeltjesverplaatsingen bepaald; evenwijdig en loodrecht op de gravitatie veld. Er werd aangetoond dat de richting van het externe gravitatieveld gekoppeld is aan het dynamisch gedrag van de deeltjes waardoor de waarden van de gemiddeld kwadratisch verplaatsing beïnvloed worden.

Het proefschrift eindigt met een samenvatting in drie talen - Engels, Nederlands en Bulgaars.

Резюме

Какво представляват колоидите, определен клас от които е обект на изучаване в тази дисертация?

Система от едно вещество (диспергирана фаза), разтворено в другото вещество (непрекъсната фаза или дисперсна среда) се нарича колоид. В колоидите, размерът на частиците на диспергирана фаза е от порядъка на от 1 до 1000 нанометра. Според вида на диспергираната и на непрекъснатата фаза, колоидете се разделят на следните няколко вида: газ в течност - пяна (бита сметана); газ в твърдо – твърда пяна (стиропор); течност в газ – аерозол (мъгла, облаци); течност в течност – емулсия (прясно мляко, майонеза); течност в твърдо – гел (желе, сирене, опал); твърдо в газ – аерозол (пушек); твърдо в течност – сол (боя, мастило); твърдо в твърдо – твърд сол (златно рубинено стъкло). Посочените примери, показват колко широко разпространени са колоидите в нашето ежедневие. Те са в основата на продукти от хранително-вкусовата промишленост – мляко, сирене, майонеза; застъпени са и в огромна част от козметичната индустрия – кремове, шампоани, лакове и гелове; в бита и строителството колоидите са широко използвани под формата на различни покрития и споиващи смески. През последните 20 години колоидите все по-сигурно навлизат и в медицината като средство за анализи; за пренос на лекарствени субстанции в организма на човек; както и като нов подход за борба с рака и вируса на СПИН.

Настоящата дисертация представя резултати от изучаването на определен вид колоиди, наречени колоидни стъкла. Ако колоидна система, която в нормално състояние е флуид (течна) бъде рязко компресирана (посредством центрофугиране или рязко охлаждане), при което обемната концентрация на частиците да достигне 0.58 обемни части, то тя преминва в състояние на колоидно стъкло (посредством, така наречения „стъклен преход”). Терминът „стъкло” в случая се обосновава от липсата на подредена (кристална) структура в този вид системи. Частиците са хаотично разпределени (също както биха били разпределени в течност), но системата притежава своиствата на привидно твърдо вещество. Частиците, използвани в описаните експерименти, са маркирани (оцветени) с флуоресцентен маркер, който

ги прави видими при облъчване със светлина с определена дължина на вълната (488 nm).

Тази дисертация представя резултати от изучаването на частичковата динамика в колоидни стъкла в присъствието и отсъствието на външно гравитационно поле. Също описва изследвания върху, т.нар., повторен стъклен преход – когато едно колоидно стъкло бъде „разтопено", след което повторно премине в стъкло. Всички експериментални резултати са получение след анализи, направени в реално време и пространство с помощтта на Сканиращ Конфокален Лазерен Микроскоп, който използва лазер като източник на светлина и позволява сканиране на пробите в дълбочина.

Глава 1 представлява общто въведение с кратък исторически обзор на колоидната наука и маркира проблемите, които се разглеждат в последващите глави. Глава 2 съдържа описание на Сканиращия Конфокален Лазерен Микроскоп като един от наи-модерните и мощни методи, използван за изследвания на биологични и колоидни системи.

В Глава 3 е представен нов аналитичен метод, които позволява директни пространствени измервания и значително удължено експериментално време. Определени участъци в пробата от флуоресцентни частици биват „осветени" при максималната мощност на лазера (2 mW). Осветяването води до нарушаване структурата на флуоресцентия маркер, което прави осветените частици „невидими". По този начин части от пробата изглеждат тъмни, а други остават флуоресциращи. Методът е аналогичен на пробиването на дупка, която в този частен случай има кубична форма и строго определени размери. С помощта на специален софтуер, се следи движението на фронта от светли частици към участъка с тъмни частици (т. нар. възстановяване на флуоресценцията след фото-осветяване). След прилагане на определен математически анализ, се получава информация за скоростта на дифузия на частицие. Средноквадратичното отклонение на частиците с времето е величината, която характеризира дифузията. Времевата скала, изследвана тук е с три порядъка по-дълга от тази достъпна с известните досега експериментални методи като динамично или статично лазерно светоразсеиване. Показано е, че твърди частици, които са в концентрация над концентрацията на „стъкления" преход, изминават средно разстояния от порядъка на един частичков диаметър за време от порядъка на 0.5 до 60 дни. Нещо повече, средноквадратичното отклонение демонстрира степенновидно поведение. .Това поведение се

различава от по-рано наблюдаваното с динамично лазерно светоразсеиване. Предполага се, че разликите могат да бъдат обяснени с разлики в гравитационните ефекти, тъй като сравняваните системи се различават единствено по плаваемост на колоидните частици.

Влиянието на гравитацията върху поведението на средноквадратичното отклонение на частиците в колоидни стъкла е изследвано по-подробно в Глава 4. Като аналитичен метод отново е приложено възстановяването на флуоресценцията след фото-осветяване. Установено е, че система, която се характеризира със стъклена структура при наличието на гравитация, демонстрира ненормална дифузия ако бъде поставена в състояние на относителна безтегловност. Показано е, че гравитацията не оказва влияние върху динамиката на системи с концентрации под тази на стъкления преход, т.е. дифузията в течни колоидни системи не се влияе от присъствието на външно гравитационно поле.

Количествен анализ на структурата и динамиката на концентрирани колоидни системи, в които потенциала на привличане между частиците е усилен чрез добавяне на неадсорбиращ полимер, е направен в Глава 5. Такива системи са подложени на вторичен стъклен преход в резултат на повишаване на концентрацията на полимера. „Топенето" на „първичното" стъкло е предизвикано от повишаване концентрацията на полимера до определено ниво, над което стопеното стъкло отново се встъклява. Показано е, че локалните промени в плътността на частиците, в резултат на привличането между тях, не са по-големи от няколко процента спрямо средната частичкова плътност.

И наи-накрая, Глава 6, изследва влиянието на гравитацията върху дифузия в стъклени колоидни системи, прилагайки експериментална установка, която позволява наблюдаване на отклоненията на частиците в две различни равнини – перпендикулярно и паралелно на гравитационното поле. Промяната в гравитационните ефекти е постигната чрез диспергиране на частиците в разтворители с различна плътност, които осигуряват различни гравитационни условия – плавателност на частиците (Архимедова сила). Показано е, че посоката на гравитационното поле влияе на частичковата динамика и променя стойностите на средноквадратичните отклонения по различен начин в перпендикулярните една на друга равнини. Казано опростено, паралелно на гравитационното поле скоростта на дифузия на частиците се ускорява, а перпендикулярно на полето се забавя.

Дисертацията завършва с кратки резюмета на английски, холандски и български.

List of publications

"Real-space fluorescence recovery after photo-bleaching of concentrated suspensions of hard colloidal spheres"
N. Simeonova and W.K. Kegel, Faraday Discussions, 123, 27, (2003), (Chapter3)

"Gravity-Induced Aging in Glasses of Colloidal Hard Spheres"
N. B. Simeonova and W. K. Kegel, Physical. Review. Letters, 93,035701, (2004), (Chapter 4)

"Devitrification of colloidal glasses in real-space"
Nikoleta B. Simeonova, Roel P.A. Dullens, Dirk G.A.L. Aarts, Volkert W.A. de Villeneuve, Henk N.W. Lekkerkerker, and Willem K. Kegel , Physical Review E 73, 041401, (2006), (Chapter 5)

"Real-space determination of particle displacements parallel and perpendicular to a gravity field in glasses of colloidal hard spheres" - to be submitted, (Chapter 6)

A few thank words for you

And here I am at the most read part of each thesis – the Thank words. I will try to keep it short and clear in difference with the texts written above. It took me a while to reach this point and here approaches the moment of closing the last page with a feeling of satisfaction, but first I would like to thank all of you: my professors, colleagues, friends and family – in the Netherlands and in Bulgaria. I will use these last couple of lines to mention a few names of people I know, people that in one or another way made appearance of this work possible, people that helped me to become the person I am today.

First of all, my deepest gratitude is for Prof.dr. Willem Kegel. Thank you Willem, for giving me the chance to perform my PhD work in such a famous and great lab as Van`t Hoff Laboratorium in Utrecht., where I had the opportunity to meet some of the living legends of Colloidal Science and to learn from them. I am thankful for your scientific support, for the knowledge you transferred to me, for teaching me how a scientist should work. A big thank for your patients and understanding. Without your help I wouldn't be sitting here, in the middle of the night, writing these lines.

My special thanks to all my colleagues from the Van`t Hoff lab. It was pleasure to work with so many bright people. Particular thanks to Prof. Henk Lekkerkerker for being my initial supervisor with an always present smile and aristocratic sense of humor, which made some of the rainy Dutch days nicer. Thanks to Ben Erne for giving me a friends hand when I arrived in Utrecht and felled like "fallen from the moon". Special thanks to Roel, Dirk and Volkert for the helpful scientific discussions and support. Big thanks to my roommates during the PhD years – Gaijsje, Maria and Ivana. It was fun to share clever thoughts with you, girls. Maria, thank you for supporting my back at the moment of my defense. It is good to know that there is no place where to fall down. Andrei – большое спасибо тебе за дружбу и за цвет, которы ты внёс в моей аспирантской жизни. Stefano, my Italian is not as good as my Russian, so you have to accept my English thank you and one grazie for being my friend, with whom I could share daily problems, worries and happiness, mixed with lazy afternoon espresso. Thank you also for flying over the Big Water and not using your parachute on the way.

Outside the lab environment I would like to thank to the big scientific “Bulgarian mafia” [1]. Dear friends, (Драго, Нина, Рени, Марко, Деница, Ефи, Петър, Анелия, Краси, Надя, Данчо, Пламен, дано не пропсукам някого), всеки от нас знае за себе си каква цена е платил за излизането си от България, затова съм сигурна, че и всеки от нас оценява какво означава нашето приятелство. Радвам се, че бяхме заедно през аспиранстките си години, че споделяхме всичко, включително и ракията ☺. Радвам се,че сме заедно и днес.

Thanks to my closest friends and colleagues I have left behind in Bulgaria, but who are with me on daily bases, thank to the internet revolution or evolution.

My next word of thanks are for the MagnaMedics team – everyone, thank you for supporting and understanding me while finishing this work. Thank you for providing me with a nice working atmosphere, mixed with brainstorming and Friday biscuits and wine – it is nice just to celebrate life.

After moving from Utrecht to Maastricht I felt like immigrating to another country again. It would be really difficult to adapt to the different Limburg habits if I haven’t met the friends I have here. Here my thanks are for my neighbors from Ireneweg 42, with whom numerous of BBQ-s were eaten. Very special thanks for my close friends Matty, Briggite and Serve. (Wie is de beste in darts ☺?) Jongens, ik ben blij dat jullie me hebben geaccepteerd en thuis laten voelen. Ik zal thuis altijd wat “rotzooi” en een brandende openhaard voor jullie hebben.

A huge thank to the friends I have met at Biopartner Center Maastricht –Patric, Georgia, Jaspar and Leon. You, people, made my working days brighter. It was fun having you around while trying to improve my language skills. And speaking about language, my special thanks are for Patric, who had to learn about colloids within 1 hour, and successfully contributed to this thesis with a Samenvatting. Thank you, Patric for being there for me.

And now one of the most difficult parts, in which I really have to skip names by that, avoiding the risk of forgetting someone. Maastricht Bulgarian community – people working at Eurocontrol (thank you for keeping Benelux sky clear ☺) and their families, as well people from the Maastricht University, from DHL, OCE and from the “Tocht Boats” (more then 30 persons). Драги мои, да знаете, че ако ви нямаше, вероятността да краснословя точно в този момент, щеше да е поне наполовина по-малка. Благодаря ви, че сме като едно голямо семеиство. Хубаво е човек да

знае, че може просто да вдигне телефона и да побъбри с някого, хубаво е и просто някой да ти се обади да попита „как си?”. С една дума – радвам се, че ви има.

And just before the end of the “thank part” I would like to thank to most important people in my life – my partner Ivan and my family. For their eyes only:

Иване, благодарение на теб съм тук и заради теб успях да стигна до края на това умотворение. Благодаря ти, че беше до мен и в добро и в лошо през изминалите години. Благодаря, че не ме остави да се откажа както нееднократно ми се е искало. Надявам се,че отсега нататък, само ще берем плодовете от постигнатото и ще се радваме на Холандското слънце, доколкото ни бъде предоставено ☺. Останалото си го знаеш

Мило мое семеиство, последните редове са специално и само за вас. Мамо и татко, благодаря, че направихте от мен човека, които съм. Благодаря, че ме отгледахте, изучихте и на много неща научихте. Надявам се да не съм ви разочаровала. Мони благодаря, че си братът, с когото мога да споделям всичко и от когото мога да получа стойностен съвет, независимо по какъв въпрос. Благодаря и за личния ти принос към крайния изглед на тази дисертация. Цъки и Хриси, радвам се,че ви имам като сестри. Лельо, благодаря за моралната и психическа подкрепа през всичките тези години. Дядо-Шефе, благодаря, че си ти. Баба, ти и Ранчото ще имат винаги своето сигурно място в спомена за едно щастливо и волно детсвто. Бабо, сжалявам, че не можа да си до мен в този радостен момент, но ще бъдеш винаги в сърцето ми. Това е за теб.

На Хари, Марийка, Ваня, Митко и Бойко благодаря, че са подкрепа и част от това прекрасно семейство. Разчитам на вас (а донякъде и на себе си) броят му да се поне удвои.

И изобщо, каквото и да напиша още тук,то няма да е достатъчно, за да опише колко ви обичам, така че с това слагам точка и предлагам да минем от теорията към практиката.

[1] A.van Blaaderen , Speech after the promotion of dr. Krassimir Velikov, 2002,Utrecht

Curriculum Vitae

Nikoleta Borissova Simeonova was born on 2^{d} of April 1976 in Sofia, Bulgaria. In 1994 she graduated in Russian Language Secondary School "St.Kliment Ohridski" in Sofia. In 1999 she obtained her M.Sc. degree in Chemistry at Chemistry Faculty of Sofia University "St.Kliment Ohridski" with specialization Theoretical Chemistry and Chemical Physics. In the period 1997 - 2000 she was working as a Research assistant at Laboratory for Chemical Physics and Engineering, Sofia University, where in 1999 she completed her Master thesis with a subject "Solubilization of triglycerides in nonionic surfactant solutions in presence of different additives". From year 2000 till 2004 she performed her PhD research at Van`t Hoff laboratory for Physical and Colloid Chemistry, Debye Institute, Utrecht University, Netherlands. In 2005 she started work at MagnaMedics Diagnostics B.V, Maastricht, Netherlands as a Research Scientist. The subject of her research and developmend are magnetic nano-particles for Life Science research; analytical laboratories; medical diagnostics and therapy applications.

HORA EST